

Nitrated fatty acids are cell membrane biochemical capacitors that regulate inflammation

Nicole Colussi¹, Sonia R. Salvatore¹, Matias M. Vazquez¹, Maria V. Gutierrez^{2,3}, Scott Hahn^{1,4}, Karina Ricart⁵, Felipe Vendrame⁵, Matias Badino¹, Agustina Schopfer¹, Dario A. Vitturi⁵, **Luis Villacorta¹⁰**, Rakesh P. Patel⁵, Amit Gaggar^{5,6}, Carsten Skarke⁷, Adam C. Straub^{1,4}, Francisco J. Schopfer^{*1,4,8,9}

¹Department of Pharmacology and Chemical Biology, University of Pittsburgh, Pittsburgh, Pennsylvania, **USA**

²Departamento de Bioquímica Clínica, Facultad de Ciencias Químicas, Universidad Nacional de Córdoba, Córdoba, Argentina

³Centro de Investigaciones en Bioquímica Clínica e Inmunología, CIBICI-CONICET, Córdoba, Argentina

⁴Heart, Lung, Blood and Vascular Medicine Institute, University of Pittsburgh, Pittsburgh, Pennsylvania, **USA**

⁵Department of Pathology, University of Alabama at Birmingham, Birmingham, Alabama, **USA**

⁶Medicine Service, Birmingham VA Medical Center, Birmingham, Alabama, **USA**

⁷Institute for Translational Medicine and Therapeutics, University of Pennsylvania, Philadelphia, Pennsylvania, **USA**

⁸Pittsburgh Liver Research Center (PLRC), University of Pittsburgh, **USA**

⁹Center for Immunometabolism, University of Pittsburgh, Pittsburgh, Pennsylvania, **USA**

¹⁰Department of Physiology, Morehouse School of Medicine, Atlanta, Georgia, **USA**

*Correspondence should be addressed to: Francisco J. Schopfer, PhD, University of Pittsburgh School of Medicine, Department of Pharmacology and Chemical Biology, E1340 Biomedical Science Tower, 200 Lothrop St., Pittsburgh, PA 15216, Phone: 412-648-0193; Email: fjs2@pitt.edu

Figures/tables: 8 main figures, 1 table, **11 supplemental figures**

Key Words: Nitro fatty acid, conjugated linoleic acid, phospholipids, lipid mediator, nitration, endotoxemia, anti-inflammatory, sepsis

SIGNIFICANCE

Lipid mediators are central regulators of inflammation, yet current paradigms largely focus on enzymatically derived oxylipins, overlooking a broader landscape of redox-derived bioactive lipids. This study identifies endogenous nitrated fatty acids (NO₂-FAs), particularly nitro-conjugated linoleic acid (NO₂-CLA), as a dynamically regulated and physiologically relevant class of anti-inflammatory mediators. We uncover complementary pathways linking dietary intake and membrane lipid nitration to NO₂-CLA formation, establishing phospholipids as a previously unrecognized reservoir that can be rapidly mobilized through phospholipase A2 activation. Once released, NO₂-CLA acts as a potent electrophilic signaling molecule that suppresses inflammatory pathways and competes with canonical pro-inflammatory lipid mediators. Notably, we demonstrate that this protective lipid pool is rapidly depleted during inflammatory stress in both murine models and human subjects, revealing a temporal dimension to its bioactivity. These findings redefine how NO₂-FAs are generated and function in vivo, bridging metabolism, redox chemistry, and immune signaling. By identifying a transient, endogenous anti-inflammatory lipid reserve that becomes depleted during disease, this work highlights a potential therapeutic opportunity to restore NO₂-CLA levels and sustain the resolution of inflammation.

HIGHLIGHTS

1. Distinct dietary and membrane-derived pathways drive endogenous formation of nitrated fatty acids (NO₂-CLA).
2. Membrane phospholipids are reservoirs for electrophilic NO₂-CLA poised for rapid signaling during acute inflammatory events.
3. Early mobilization of NO₂-CLA functions as a brake on pro-inflammatory signaling, reducing cytokine release and hypotension.
4. Dietary consumption of CLA and nitrite could boost post-injury restoration of protective NO₂-CLA pools.

28

29 **SUMMARY**

30 Endotoxemia triggers the rapid synthesis of bioactive lipid mediators through enzymatic
31 and radical-mediated mechanisms. Among these, nitrated fatty acids (NO₂-FAs) form by
32 nitration reactions and function as anti-inflammatory signaling lipids. Although their therapeutic
33 potential in inflammatory diseases is well established, integrated NO₂-FA signaling in the context
34 of endogenous formation remains unexplored. Herein, we humanize cellular and mouse fatty
35 acid profiles with conjugated linoleic acid to study the predominant lipid sources and protective
36 responses of endogenous nitro-conjugated linoleic acid (NO₂-CLA) during endotoxemia. We find
37 that phospholipids are functional biochemical capacitors, capable of storing diet-derived NO₂-
38 CLA under basal conditions and completely releasing it during acute inflammatory responses,
39 resulting in decreased cytokine production and improved vascular homeostasis. These findings
40 were validated in samples from septic patients and volunteers treated with lipopolysaccharide
41 as a model of systemic aseptic inflammation. The work reported here delineates the synthesis,
42 metabolic fate, and immunomodulatory capacity of endogenous NO₂-FAs.

43

INTRODUCTION

Lipid metabolism contributes to the complex pathophysiology of inflammation by generating pro-inflammatory and counter-regulatory mediators, whereby the rate-limited hydrolysis of fatty acids by phospholipase A2 (PLA2) governs their bioavailability^{1,2}. Following release from the sn-2 position of phospholipids, fatty acids directly engage G-protein coupled receptors (GPCR) or are rapidly converted into stereoselective, oxidized derivatives by cyclooxygenase (COX), lipoxygenase (LOX), and cytochrome P450 (CYP450) epoxygenase for subsequent target activation and inflammatory signaling^{3,4}.

Despite their assignment as the canonical lipid mediators, oxylipins derived from the enzymatic oxidation of arachidonic acid (AA) and omega-3 polyunsaturated fatty acids (PUFAs) incompletely represent the total pool of bioactive lipids. Free radical-driven lipid peroxidation and nitration reactions generate diverse species that transduce redox signals by participating in reversible and irreversible protein modifications⁵⁻⁹. Oxidants, including hydroxyl radical ($\bullet\text{OH}$), hydroperoxides (ROOH , H_2O_2), and nitrogen dioxide ($\bullet\text{NO}_2$), serve as radical initiators for these reactions, and the double bond configuration of unsaturated fatty acids dictates the final product distribution¹⁰. In this regard, there has been a recent emphasis on evaluating the strikingly different reactivities and products of bisallylic and conjugated fatty acids with cellular oxidants^{11,12}. Their differential behavior becomes increasingly relevant with $\bullet\text{NO}_2$ exposure, as this radical mainly induces lipid peroxidation in reactions with bisallylic fatty acids [e.g., linoleic acid (LA)] but forms thiol-reactive electrophilic nitroalkenes when reacting with conjugated fatty acids [e.g., conjugated linoleic acid (CLA)]¹³⁻¹⁹. Radical reactions that favor the generation of $\bullet\text{NO}_2$ are widespread, predominantly occurring in the acidic stomach compartment and cell membranes by the decomposition of nitrous acid and nitric oxide ($\bullet\text{NO}$) autooxidation, respectively^{20,21}. Hence, dietary triglycerides and membrane phospholipids are proposed as major substrates for nitrated fatty acid ($\text{NO}_2\text{-FA}$) formation.

The first description of the endogenous formation of NO₂-FAs was made using a rodent model of *in vivo* ischemia-reperfusion injury²². Following this initial report, years of intensive characterization efforts failed to reveal bisallylic fatty acid nitration in biological systems, eventually showing that conjugated fatty acids are primary targets for nitration due to the resonance stabilization of obligatory reaction intermediates¹⁴. CLA is the most abundant and studied conjugated fatty acid in humans, primarily obtained from ruminant dairy and meat products in the form of *cis*-9, *trans*-11 CLA²³. As a minor route, the isomerization of LA and desaturation of vaccenic acid by microorganisms in the human gut also contribute to endogenous CLA levels²⁴⁻²⁶. Nitrite provided by the diet and the salivary glands in the presence of dietary CLA promotes, through the acidic pH of the stomach, the synthesis of nitro-conjugated linoleic acid (NO₂-CLA). While levels can be monitored in the plasma, greater than 30% of lipid nitration products and metabolites are excreted into urine, making it an ideal matrix for assessing NO₂-FA formation and metabolism. Of the total NO₂-FAs detected in human urine, NO₂-CLA accounts for 60% of the nitrolipidome²⁷. Alongside basal formation via gastric synthesis, it is expected that membrane lipid nitration yields NO₂-FAs under conditions of inflammation or nitro-oxidative stress.

•NO is a highly diffusible radical, and hydrophobic compartments accelerate the autoxidation of •NO by 30×, thereby exposing membrane lipids to high concentrations of •NO₂²¹. Given the quenching behavior of membranes and favorable radical milieu, phospholipid nitration is envisioned to be highly efficient during pathological events involving elevated •NO synthesis and signaling, thereby contributing to NO₂-CLA formation.

Once generated by dietary or localized radical reactions, NO₂-CLA may regulate diverse cell responses by modulating redox signaling pathways, gene transcription, and enzymatic activity of target proteins^{9,28}. Mechanistically, electrophilic NO₂-FAs reversibly alkylate nucleophilic amino acids by Michael addition reactions, post-translationally altering the function of redox-sensitive proteins and transcription factors^{29,30}. Notable targets include the inhibition of pro-inflammatory NF-κB, cGAS-STING, calcineurin, STAT3 pathways, and activation of the antioxidant (Nrf2-

Keap1) and heat shock protein (HSP) response³¹⁻³⁶. Capitalizing on these protective phenotypes, the synthetic 10-nitro oleic acid (10-NO₂-OA) was developed and demonstrated safety and biomarker engagement in five Phase I clinical trials and is currently in Phase II clinical trials for the treatment of obese asthma (NCT03762395).

Despite the analytical and technical advances in the field, significant challenges remain. Evaluating the endogenous formation of NO₂-FAs in cells and animal models has been mostly limited to direct administration of CLA to macrophages or sites of inflammation to provide evidence of endogenous nitration^{32,37}. This approach precluded a thorough *in vivo* assessment of their synthesis, signaling, and metabolism under biologically relevant pathophysiological conditions. Herein, using newly developed cellular and mouse models, we reveal distinct yet complementary nitration routes, establishing the considerable value of dietary NO₂-CLA synthesis. We found that phospholipids in cellular membranes predominantly serve as a reservoir for NO₂-CLA, providing a ready-to-engage pool of anti-inflammatory lipids. Upon PLA2 activation, NO₂-CLA is rapidly converted into the signaling-active free acid, which antagonizes inflammatory signaling cascades and competes with pro-inflammatory mediators derived from oxylipin and prostaglandin synthesis. This early release exhausts cellular stores of NO₂-CLA, effectively protecting against sepsis-induced cytokine release and hypotension. These findings were recapitulated in human samples obtained from healthy subjects receiving lipopolysaccharide (LPS) or from ICU patients with sepsis and septic shock. The rapid depletion observed in humans subjected to sterile or infectious inflammation provides mechanistic insights into the temporal action of pharmacological NO₂-FAs and highlights the potential need for replenishing this pool of non-canonical anti-inflammatory lipids for sustained protection.

RESULTS

CLA supplementation primes cellular and in vivo systems for lipid nitration

NO₂-CLA is detectable in human urine at varying concentrations, whereas the contrary is observed in cultured cells and rodents^{27,38}. The evaluation of lipid nitration and basal levels in cell

and rodent models has proven challenging, consistently leading to analytical failures and greatly limiting the available models for studying these bioactive lipids. An analysis of culture media, mouse tissue, and rodent chow confirmed an absence or negligible levels of CLA (Supplementary Fig. 1). Deficiency in vaccenic acid and CLA, the only sources of conjugated fatty acids, explains its absence in animal tissues and cells in culture and significantly limits the substrate for NO₂-CLA formation.

To address this shortcoming, we developed cellular and *in vivo* models that better reflect human CLA compositions by supplementing this nitration substrate. Under basal conditions, CLA free and esterified levels were below the limit of quantification (~3 pmoles/million cells) in RAW264.7 macrophages cultured in 10% fetal bovine serum (FBS), as assessed by gas chromatography-mass spectrometry (GC-MS). Supplementation with BSA-complexed CLA (50 μ M) increased the esterified levels to 9%, while the free acid levels remained very low (Fig. 1A, B and Supplementary Fig. 2A). This increase in CLA did not significantly modify the typical fatty acid distribution of macrophages, except for slight decreases in oleic (18:1) and palmitoleic acid (16:1), which is consistent with reports of CLA-inhibition of stearyl-CoA desaturase (SCD1) in culture conditions (Supplementary Fig. 2A)^{39,40}. We next evaluated the position of CLA incorporation into phospholipids by hydrolysis using phospholipase A1 and A2 (PLA1 and PLA2). CLA was detected in both positions after phospholipase treatment, aligning with the chain distribution reported previously (Supplementary Fig. 2B)⁴¹. Depending on the isomer, CLA is esterified in the sn-2 position, which is consistent with a role in inflammation since sn-2 PUFAs are released by PLA2.

Although conjugated fatty acids are primarily obtained from the diet, CLA is available as a nutritional supplement for healthy body composition and tone. Based on the recommended daily dose (3 g/day) for human subjects, we used allometric scaling to calculate the equivalent dose for CLA supplementation in mice (0.7%) and selected a 1% CLA diet that replaced 1% of LA (control diet, negative control for endogenous nitration products). This dietary intervention to humanize fatty acid profiles was maintained for 4 weeks (Fig. 1C). As previously reported, the

CLA-enriched diet led to a whole-body fat redistribution from adipose tissue to liver, trending to a lower overall bodyweight (Supplementary Fig. 3A, B)⁴²⁻⁴⁴. Fatty acid tissue incorporation was quantified by GC-MS, as it resolves CLA from LA in control and treated tissues (Fig. 1D). Heart and kidney showed the highest CLA incorporation, reaching about 3% of the total fatty acid pool, with lower levels in spleen, liver, and lung (Fig. 1E). Importantly, the CLA treatment did not alter the fatty acid profiles in the tissues studied (kidney, Fig. 1F, G; heart, spleen, liver and lung, Supplementary Fig. 3C, D), while the total level of LA remained stable or slightly decreased (Supplementary Fig. 3E).

The incorporation of CLA isomers into major complex lipids has been previously evaluated in mouse liver and human serum after separation of classes by thin-layer chromatography. Across these studies, triglycerides consistently represented the predominant reservoir of CLA isomers after supplementation⁴⁵⁻⁴⁷. To contextualize the CLA tissue incorporation in our 1% dietary model, lipid classes from liver, kidney, and lung were fractionated to isolate phospholipids, triglycerides, and cholesterol esters. Spleen and heart tissue were not available for lipid assessments. Separation of lipid classes was confirmed with HPLC-CAD-MS, and fractions were hydrolyzed, derivatized, and fatty acids evaluated using GC-MS (Supplementary Fig. 4). We found a low enrichment of CLA, ranging from 1 to 5% (Supplementary Fig. 5). CLA was mostly enriched in triglycerides in kidney and lung tissue and in phospholipids in the liver. Although concentrations differed slightly from those reported in the literature, the trend remains consistent with triglycerides as the predominant source of CLA. Overall, we established and characterized an appropriate model to study endogenous lipid nitration and metabolism *in vitro* and *in vivo*.

Oral CLA administration increases NO₂-CLA in a murine model

In the intestinal lumen, enterocytes absorb orally delivered NO₂-OA, which is incorporated into chylomicrons and secreted into lacteals and the lymphatics before reaching the systemic circulation⁴⁸. Given their structural similarity, NO₂-CLA formed in the acidic stomach compartment should follow a similar path as previously reported for NO₂-OA, including systemic distribution and

further metabolism into inactivated derivatives, β -oxidation products, or conjugates with cellular thiols (Fig. 2A)⁴⁹⁻⁵¹. After 4 weeks of CLA supplementation, NO₂-CLA, the reduced metabolite dihydro-NO₂-CLA (red-NO₂-CLA), and GSH-NO₂-CLA are readily detectable in plasma (Fig. 2B). Analytical standards were used to correctly identify endogenous nitration products in the LC-MSMS chromatographic traces, where peaks eluting after the selected areas represent artifacts of non-covalent adducts between fatty acids and nitrite (grayed out traces)⁵². These nitration products and metabolites remained undetectable in mice receiving the LA diet (Fig. 2B). On average, NO₂-CLA as a free acid was found in plasma at 5 nM (0-11 nM range), a level close to the reported basal circulating concentration in healthy human volunteers (1-2 nM), which increases to 8-15 nM upon NO₂- and CLA oral administration⁵³. The concentration obtained in this study after human supplementation is comparable to the 10-NO₂-OA levels reached upon administration of the selected therapeutic doses used in clinical trials (150 mg/day, C_{max} 7.5 nM), highlighting the signaling potential of endogenous NO₂-CLA levels^{53,54}. Upon plasma lipid hydrolysis, mean levels in mice increased nearly 2-fold, contributed by TG esterified NO₂-CLA, reaching up to 17 nM. Levels of reduced NO₂-CLA (red-NO₂-CLA) also increased upon hydrolysis (Fig. 2C).

In tissues from CLA-fed mice, NO₂-CLA did not correlate with CLA levels, revealing tissue-specific differences in NO₂-CLA uptake, metabolism, and disposal that are independent of consumed CLA. The heart and kidney showed a weak association between the total levels (free plus esterified) of CLA and NO₂-CLA, whereas there was no relationship in the liver, lung, and spleen (Supplementary Fig. 6A). A linear relationship becomes more apparent for all tissues when comparing total CLA and red-NO₂-CLA (Supplementary Fig. 6B). This data shows that the inactive metabolite may serve as a better biomarker for total nitration than the reactive NO₂-CLA, as its levels fluctuate less. Nonetheless, this “snapshot” of tissue levels for both NO₂-CLA and red-NO₂-CLA levels after 4 weeks on the CLA diet provides an appropriate representation of the steady state of systemic nitroalkenes that includes the effects of distribution, metabolism, and elimination.

NO₂-FAs are mainly excreted as cysteine adducts in urine; thus, urine samples were treated with mercury chloride to reverse the modification and enhance detection before LC-MSMS assessment²⁷. Like native fatty acids, these bioactive mediators are substrates for mitochondrial β -oxidation, generating truncated derivatives that retain their electrophilic character⁶. Urine LC-MSMS traces from mice receiving the CLA diet showed the main β -oxidation metabolites for NO₂-CLA, including NO₂-16:2 (dinor-NO₂-CLA), NO₂-14:2 (tetranor-NO₂-CLA), and NO₂-12:2 (hexanor-NO₂-CLA) (Fig. 2D). In line with previous work, these species were highly prominent in urine with levels reaching up to 6 nmol/mg creatinine for NO₂-14:2 (Fig. 2E)^{27,38}. Notably, NO₂-CLA was the least abundant of the urinary NO₂-FAs, but its concentration strongly correlated with the downstream metabolite levels, affirming NO₂-CLA as the sole precursor in mice (Fig. 2F). Despite the concentration observed in the urine, these electrophilic metabolites were not detected in the plasma, supporting a significant role for the renal metabolism of NO₂-FAs. Importantly, the detailed characterization of the endogenous formation and metabolism of NO₂-CLA in our rodent model shows a close correlation with the levels observed in human volunteers, highlighting the translational potential of pathophysiological findings derived from this system.

Phospholipids are biochemical cell capacitors that store endogenous NO₂-FAs

In cells, NO₂-FAs are stored as esterified species in complex lipids, forming a poorly understood pool that is protected from metabolism and chemical degradation^{55,56}. **Given that CLA is available in neutral lipids and phospholipids, we evaluated the distribution of endogenous NO₂-CLA amongst these species. Using solid-phase fractionation, we separated and quantified lipid classes from kidney, liver, and lung by HPLC-CAD-MS (Supplementary Fig. 4). Subsequently, we hydrolyzed the fractions and quantified NO₂-CLA by HPLC-MSMS. In contrast to our CLA findings, we established that for these three tissues (liver, lung, and kidney), the phospholipid fraction contained the highest level of NO₂-CLA, followed by triglycerides. Levels enriched in the cholesterol ester pool were below the LOQ (Fig. 3A). The preferential placement of signaling-active NO₂-CLA in phospholipids indicates participation in the Land's cycle, a remodeling process**

that controls incorporation, composition, and positional stereochemistry in phospholipids (Fig. 3B)⁵⁷. This process mirrors oxylipin metabolism and provides a mechanism for the esterification of NO₂-CLA in the sn-2 position for release by PLA2 during inflammatory challenge⁵⁸. To further evaluate the suitability of NO₂-CLA for selective incorporation into phospholipids, we measured NO₂-CLA coenzyme A conjugates (NO₂-CLA-CoA) in RAW264.7 macrophages. Fatty acid coenzyme A conjugates are substrates for Acyl-CoA:lysophosphatidylcholine acyltransferase (LPCAT), which is one of four enzymes responsible for phospholipid remodeling⁵⁷. The detection of the formation of NO₂-CLA-CoA adducts in RAW264.7 macrophages following NO₂-CLA treatment (Fig. 3C) supports a role for this key metabolite in the incorporation and storage of this anti-inflammatory lipid in membranes that can initiate early responses to inflammatory stimuli.

In addition to functioning as a selective reservoir for pre-formed NO₂-CLA, phospholipids have been discussed as targets for nitration during inflammation or dysregulated redox status⁵⁹⁻⁶². Given the significant contributions of inducible nitric oxide synthase (iNOS) and •NO in the development of inflammation and sepsis, it has been proposed that CLA esterified in cell membranes will react efficiently with •NO₂ to drive NO₂-CLA synthesis. Nitric oxide-mediated nitration of free CLA in media has been previously shown in activated RAW264.7 macrophages³⁷. Although this model demonstrated the capacity to nitrate free acid CLA by the inflammatory conditions, it does not address CLA nitration in phospholipids or its release by PLA2, nor does it model physiological conditions where free acid CLA levels are orders of magnitude lower than esterified CLA. To characterize this cascade, we used the supplemented cell model to determine whether membrane esterified CLA is a substrate for nitration in RAW264.7 macrophages activated with LPS and IFN γ (Fig. 3D). Endotoxin challenge led to the formation of NO₂-CLA, with 71% of the total nitroalkene pool found esterified and the remaining adducted to thiols (Fig. 3E). The nitration of phosphatidylcholine-esterified CLA was blunted with iNOS inhibition (Fig. 3F) and absent in LA-supplemented controls (Supplementary Fig. 7), affirming that CLA effectively diverts •NO-derived oxidants to NO₂-CLA formation with anti-inflammatory capabilities. Since free CLA

levels following supplementation are extremely low (below level of quantification, LOQ), NO₂-CLA formation is most likely occurring in the membrane compartment and PLA2 hydrolysis must occur before further metabolism and engagement with cellular thiols. Thus, the presence of reduced and β -oxidized metabolites in membrane phospholipids as evaluated by high-resolution LC-MS (Fig. 3G, Table 1) can only be explained by an active Land's cycle (Fig 3B), whereby NO₂-CLA is released, metabolized, and then metabolites re-esterified into PCs. In aggregate, we have demonstrated that phospholipids play a unique dual role in the storage and formation of endogenous fatty acid nitroalkenes.

Endotoxemia favors the net loss of NO₂-CLA

To translate our cellular model of NO₂-CLA formation into a murine model, we challenged mice with LPS for 16 hours after 4 weeks of CLA supplementation (Fig. 4A). Previous *in vivo* studies following the nitration of CLA during endotoxin or viral inflammation relied on a bolus administration of free acid immediately before challenge, and NO₂-CLA was measured locally in the exposed compartment³². With our CLA-enriched model, we assessed changes in tissue concentrations of NO₂-CLA, expecting increased total (free and esterified) NO₂-CLA levels due to inflammation-driven nitration of phospholipids, which amplify the basal contributions of dietary nitroalkene esterification both in phospholipids and TGs (Fig. 4B). Upregulation of iNOS is achieved as early as 4 hours with LPS-mediated endotoxemia, therefore 16 hours was selected to capture the accumulation of NO₂-CLA and compared to responses in LA-supplemented mice⁶³.

Even with CLA being available in tissue compartments at physiologically relevant concentrations for nitration, we observed a significant net loss of NO₂-CLA in heart, lung, and liver tissues from LPS-challenged mice receiving the CLA diet (Fig. 4C). The lung was the most sensitive to inflammation-driven nitroalkene loss, showing a 5-fold reduction in NO₂-CLA. Moreover, the spleen and kidney appear to be more resistant to NO₂-CLA depletion since levels are relatively unchanged between CLA-fed controls and challenged mice. The differences between tissues may reflect their ability to mobilize (or generate) NO₂-CLA during inflammation.

Similar to the active nitroalkene, red-NO₂-CLA levels were also lower in the heart, lung, and liver of CLA-fed mice receiving LPS, with lung tissue showing again the strongest decline (4-fold reduction) (Fig. 4D). We next evaluated if β -oxidation of NO₂-CLA was responsible for the decreased overall levels, as this is a major metabolic pathway to dampen the activity of oxylipins⁵⁸. Although readily measured in urine (Fig. 2F), these truncated metabolites were below the limit of detection (LOD) in tissues and remained undetectable in mice challenged with LPS. As another potential source of NO₂-CLA, we assessed whether the pool of nitroalkenes shifted toward the formation of thiol adducts after release from membranes. As a free acid, calculations based on the equilibrium constant indicate that, under steady state conditions, >99% is covalently conjugated to cellular thiols⁶⁴. Again, we observed a generalized decrease in the total levels of adducted NO₂-CLA (Fig. 4E). It is important to note that the mercury-based thiol exchange method used to quantify adducted NO₂-CLA only captures products of reversible kinetic addition reactions⁵¹. Eventually, these reversible adducts are expected to trans-alkylate into glutathione given its cellular abundance (8-14 mM) to support its cellular export or shift towards slowly reacting with nucleophiles that have a higher k_{eq} , displacing the equation toward products and supporting the formation of more stable, thermodynamic products⁵¹. After de-esterification, nitroalkylation may favor the irreversible thermodynamic product over time, but current analytical methods based on mercury exchange reactions cannot access this subset of thiol reactions (1,4 addition products) or potential histidine conjugates^{38,51}. Importantly, the two analyzed tissues that had no detectable thiol adducts (kidney and spleen) had no changes in esterified NO₂-CLA levels.

To better characterize the nitration of CLA in phospholipids, a second cohort of mice was challenged with LPS for 6 hours. Although not as definitive, there is still a decrease in total NO₂-CLA, red-NO₂-CLA, and NO₂-CLA thiol adducts in CLA-fed mice receiving LPS compared to those receiving the saline vehicle at 6 hours (Supplementary Fig. 8A-C). As observed at 16 hours, kidney and spleen showed no changes in esterified NO₂-CLA and red-NO₂-CLA levels, supporting a different regulatory mechanism in these organs. This lack of change in membrane levels is

reaffirmed by no detectable levels of adducted NO₂-CLA. Overall, tissues that display an active net loss of diet-derived NO₂-CLA do not reveal the expected counteracting response of NO₂-CLA synthesis under the inflammatory challenge. While previous efforts worked under the assumption that LPS would increase NO₂-CLA levels due to upregulated iNOS expression, it may be possible that iNOS induction is lower in parenchymal cells than in macrophages or monocytes. Moreover, with the concomitant increase in superoxide formation from NADPH oxidases normally seen during endotoxemia, then the ability of •NO to diffuse into parenchymal cells might be significantly decreased⁶⁵. Therefore, levels in tissue reflect de-esterification without a significant contribution of inflammatory NO₂-CLA formation, providing a timely release of an efficient anti-inflammatory agent that overwhelms any simultaneous de novo synthesis during the initial stages of inflammation.

NO₂-CLA inhibits the release of sn-2 esterified fatty acids

LPS binds to Toll-like receptor 4 (TLR4) to induce a signaling cascade that leads to cPLA2 phosphorylation and activation, hydrolyzing fatty acids from the sn-2 position of phospholipids. The hydrolysis of fatty acid substrates is an early event that contributes to a full inflammatory cellular response through the synthesis of oxylipins and eicosanoids, which can be monitored in the plasma^{2,58}. Following the observed net loss in tissue, we assessed the extent of NO₂-CLA release by measuring levels of free nitroalkene in the plasma from LPS-challenged mice. The de-esterification of NO₂-CLA is not captured in the plasma at 6 hours, but levels fall below the LOD by 16 hours. Conversely, the red-NO₂-CLA inactive metabolite is detectable late in the inflammatory cascade (Fig. 5A).

The acute IV administration of 10-NO₂-OA rapidly interferes with LPS-induced TLR4 signaling by inhibiting the recruitment of TLR4 into lipid rafts and disrupting the assembly of adaptor proteins upstream of NF-κB activation⁶⁶. We asked if the rapid hydrolysis of NO₂-CLA from the membranes could inhibit the early LPS inflammatory response and the synthesis of relevant lipid mediators. To assess changes in the plasma lipid profile, an untargeted LC-MSMS

analysis was performed. The volcano plot generated by the differential analysis between LA- and CLA-fed mice after 6 hours of LPS challenge showed highly significant downregulated lipid species in the CLA group (Fig. 5B). NO₂-CLA was not identified in this study due to the intrinsic instrument sensitivity limitations of screening approaches. Using the Lipids Maps online database, the modulated components were identified and manually validated, revealing free fatty acids and dihydroxy fatty acids as the most frequent modified class (Fig 5C). The prototypical sn-2 FA constituents, including α -linolenic acid (ALA), eicosapentanoic acid (EPA), arachidonic acid (AA), and docosahexaenoic acid (DHA), increased 3- to 5-fold in the plasma 6 hours after LPS administration and returned to baseline at 16 hours (Fig. 5D). CLA supplementation did not affect the basal levels of these fatty acids, but significantly dampened this response, supporting an early inhibition of inflammatory activation processes. To control for unspecific lipolysis and release of fatty acids from phospholipid and TG stores, we profiled the saturated palmitic (PA) acid and stearic acid (SA), as they are mostly enriched in phospholipid sn-1 positions and TGs. Their plasma concentration remained constant with no significant differences observed between the CLA and LA groups (Fig. 5E).

Dihydroxy fatty acids are one cluster of bioactive lipids synthesized primarily by the CYP enzymes or obtained as downstream metabolites of LOX activity. Like their fatty acid precursors, dihydroxy DHA (DiHDHA) and AA (DiHETE) are reduced in the plasma of CLA mice, whereas dihydroxy DPA (DiHDPA) remains comparable between the diet groups (Fig. 5F). However, these oxidation products are not strongly induced by LPS challenge. DiHETE showed the greatest change, doubling with LPS challenge which is consistent with other reports for this oxylipin⁶⁷. Extending to alternative oxylipins, we saw no changes in total HETEs (hydroxy eicosatetraenoic acids) over the course of LPS challenge, and total HODEs (hydroxy octadecadienoic acids) only showed a 2-fold elevation by 16 hours in both LA- and CLA-treated mice (Supplementary Fig. 9A, B). The failed upregulation for these canonical products aligns with other studies showing that LPS challenge to mice does not stimulate overwhelming changes in circulating LOX, COX, and

CYP products, for around 2-3-fold changes in LA and AA oxidation species are usually reported unless metabolism pathways are inhibited^{58,67,68}. Even though these oxidation products are not profoundly elevated during endotoxemia, NO₂-CLA still serves as any early modulator of inflammation, attenuating the release of fatty acid precursors and synthesis of dihydroxy fatty acid species.

Human urine accumulates excreted NO₂-CLA after LPS administration

Oxylipin metabolism is best evaluated by urinary analysis, and the same applies to NO₂-FAs⁶⁹. Thus, we decided to evaluate the temporary profile of NO₂-CLA and its main metabolites in urine from healthy human volunteers who were challenged with a low dose of endotoxin as part of a previously published clinical study to evaluate systemic inflammatory responses⁷⁰. Urine samples were collected serially from 35 human subjects throughout their inpatient visit at the following time intervals: 0-2 hours, 2-4 hours, 4-6 hours, and 12-18 hours. Acute inflammation leads to an elevation in urinary NO₂-CLA over time (Fig. 6A). To further dissect the metabolic profile on an individual level, we used paired analyses to compare trends between the first and second half of the endotoxin challenge. Most participants exhibited slight reductions in urinary NO₂-CLA during the first 6 hours of endotoxin exposure, with levels increasing in the last collection period (Fig. 6B). Without de-esterification by PLA2 or de novo synthesis, the urinary levels of nitroalkenes are expected to decrease in a time-dependent manner, as observed previously in humans after oral administration of CLA and nitrite⁵³. However, the observed accumulation of NO₂-CLA in urine by 12-18 hours after LPS administration is consistent with an increased net release from phospholipid stores (or any de novo synthesis). Next, we assessed whether levels of truncated metabolites of NO₂-CLA were elevated in the urine over the course of inflammation. Electrophilic, β -oxidized derivatives of NO₂-CLA strongly decreased within the first 6 hours, with NO₂-16:2 being the only metabolite that accumulated in urine by 12-18 hours (Fig. 6C, D). Given the lack of formation of NO₂-14:2 and NO₂-12:2 products, β -oxidation may not be the favored

metabolic route for nitroalkenes during inflammation (Fig. 6E-H). Additional metabolites reported for NO₂-FA include ω -oxidation, with taurine conjugation and sulfation being predominantly found in rodents⁷¹. While these are not the most abundant metabolites, further analysis may be required to better understand the impact of inflammation on NO₂-CLA metabolism.

Endogenous NO₂-CLA attenuates pro-inflammatory cytokines and regulates vascular responses

NO₂-CLA exerts anti-inflammatory actions at multiple levels in the inflammatory cascade, including in TLR4, NF- κ B, Calcineurin, STING, and STAT3 signaling, with these supporting the rationale for the therapeutic development of 10-NO₂-OA^{31-34,66}. Therefore, we wanted to evaluate whether the CLA administration had an impact on inflammatory outcomes *in vivo*. As cytokines are maximally elevated between 4-8 hours after LPS administration, we assessed their circulating levels at 6 hours using a multiplex panel⁷². TNF α , IL-6, IL-17, and IL-5 are highly upregulated with LPS administration, and CLA dietary supplementation significantly decreases their circulating levels (Fig. 7A). Additional cytokines trend lower, including IL-1 β , IL-12, IFN γ , and MCP1, but did not reach significance. Notably, IL-10, a cytokine involved in the resolution of inflammation, remains unchanged with CLA supplementation. By 16 hours, plasma cytokines start to resolve, but some, including MCP-1 and IFN γ , are marginally elevated for the CLA group compared to LA (Supplementary Fig. 10). To confirm the effect of NO₂-CLA on the cytokine profile, we activated RAW264.7 macrophages and evaluated the transcription of IL6 and IL-1 β mRNA. Both are significantly inhibited in the CLA-supplemented group compared to LA-supplemented controls (Supplementary Fig. 11A). In addition, there is a reduction in IL-6 levels in the supernatant in the macrophages treated with CLA (Supplementary Fig. 11B), all of which are consistent with previous observations showing a potent inhibition of LPS-induced inflammation in RAW264.7 macrophages by NO₂-CLA³⁷.

Since declines in vascular tone are observed in endotoxemia due to excessive •NO production and vascular dysfunction, we wanted to assess whether NO₂-CLA formed by the consumption of CLA diet prevented the hypotensive effects of LPS. Telemetry devices were implanted into LA- and CLA-fed mice to obtain continuous blood pressure measurements before and following intraperitoneal LPS challenge. While both groups display the characteristic decrease in baseline blood pressure around 4 hours after LPS administration, the CLA group shows a significant protection from vasorelaxation, with differences of up to 30 mmHg (Fig. 7B). In summary, CLA-supplemented mice are protected from inflammatory activation via signaling modulation by NO₂-CLA.

Plasma NO₂-CLA is lower in humans with septic shock

Next, we explored the change in NO₂-CLA in human sepsis. Plasma was collected from healthy subjects, non-septic ICU patients, or patients with sepsis or septic shock. In close alignment with our mouse results, total free fatty acids were significantly increased in the plasma of sepsis or septic-shock patients compared to healthy controls (Fig. 8A). In contrast, sepsis and septic shock patients showed a depletion of free levels of NO₂-CLA (Fig. 8B). The observation that NO₂-CLA was maximally decreased in both sepsis and septic shock patients vs. ICU controls further suggests that NO₂-CLA is an early target after initiation of inflammation with these changes sustained in patients that progress to septic shock. Considering that these sample collections correspond to later stages of the inflammatory responses, the findings are in close agreement with the profiles observed in mouse plasma after 16 hours of LPS (Fig. 5A). Moreover, they align with a recent report showing a significant decrease in plasma NO₂-CLA and red-NO₂-CLA and urine NO₂-CLA from patients with sickle cell disease⁷³. For free red-NO₂-CLA, there are no significant changes between healthy controls and sepsis patients (Fig. 8C). Overall, these results indicate that in sepsis, likely via PLA2, NO₂-CLA is depleted early during infections from phospholipid stores. These results also suggest that NO₂-CLA consumption pathways dominate

over endogenous formation of NO₂-CLA via elevated reactive nitrogen species, at least during the acute phase of sepsis / septic shock.

DISCUSSION

The early phase of endotoxemia is characterized by rapid activation of innate immune responses and profound metabolic reprogramming, which together shape the trajectory of systemic inflammation and tissue injury. Responses are instigated by the mobilization of fatty acids from cellular lipid stores and membranes through the activation of phospholipases and lipases. The released free FAs serve as bioactive mediators, providing substrate for lipid signaling pathways and eicosanoid synthesis. Moreover, the composition and kinetics of release can influence toll-like receptor signaling, inflammasome activation, and the overall innate immune response. Therefore, the timing, magnitude, and identity of lipid species released during the initial phase of endotoxemia are critical to understanding the regulation of the early inflammatory response. Herein, we established a novel mechanism for the regulation of inflammatory responses by CLA that involves the rapid mobilization of diet-derived, pre-formed NO₂-CLA present in **cell** membranes. These findings modify the current dogma, which proposes that de novo synthesis of NO₂-CLA as a consequence of increased oxidative and nitrative stress is the main component of their protective and anti-inflammatory effects^{22,32,37}. Unlike isolated systems supplemented with CLA, we observed a rapid net decrease of NO₂-CLA in most tissues analyzed from mice (Fig. 4), and this loss correlated with an increase in renal NO₂-CLA elimination (Fig. 6).

Dynamic changes in lipid mediators and downstream signaling are a key process by which tissues adapt to acute inflammation and return to homeostasis. This process can be changed by pharmacological interventions, genetic manipulation, and by modifying the fatty acid membrane composition. In particular, dietary interventions based on omega-3 fatty acids have been related to lower inflammation and resolution, while omega-6 diets that increase levels of arachidonic acid were found to be detrimental⁷⁴⁻⁷⁶. Several studies in mice have evaluated the anti-inflammatory effects of CLA, showing a reduction in colonic inflammation, cytokine formation, and inflammatory

mediators such as prostaglandins, leukotrienes, and immunoglobulins^{26,77,78}. Despite this promising preclinical evidence, human studies have not consistently demonstrated anti-inflammatory benefits of CLA supplementation; differences in isomer composition, target population, pathological condition, and duration of treatment have been considered as determining factors in these discrepant responses⁷⁹⁻⁸¹. An additional source of variability might be the microbiome metabolism of LA, CLA and NO₂-CLA. While the main source of CLA is dairy products, LA can also be metabolized to CLA and vaccenic acid, a precursor of CLA in the gut²⁴. Nonetheless, it has been shown that the microbiome does not significantly impact circulating and tissue CLA levels⁸². Another possibility is that the microbiome metabolizes NO₂-CLA formed during digestion. In this regard, the majority of CLA and NO₂-CLA absorption is expected to occur in the duodenum and jejunum, while the majority of the microbiome-dependent metabolism of fatty acids (saturation, oxidation) is located downstream in the colon⁴⁸. Thus, the microbiome is expected to have a small impact on CLA and NO₂-CLA levels. While we report a substantial increase in tissue NO₂-CLA in mice with daily intake of CLA, dietary and salivary levels of nitrite predominantly define gastric nitroalkene formation^{53,83}. In this regard, our previous findings in rodents and humans indicate that the intake of nitrate and nitrite is a major determinant in NO₂-CLA formation and systemic levels. These environmental and dietary factors have not been previously considered when evaluating CLA effects. Hence, NO₂-CLA levels and dietary intake of nitrite and nitrate (e.g., leafy vegetables) should be considered when studying CLA responses in clinical trials.

The detection of NO₂-FAs in rodents under physiological conditions has been extremely challenging, in part due to the low endogenous levels and small sample volume (e.g., urine, plasma). Moreover, the gastric environment was not considered to be conducive to NO₂-CLA formation due to a higher pH than humans (~5 vs 1.5)⁸⁴. Thus, to elicit biological responses, gavage of CLA and nitrite was previously co-administered with pentagastrin to further reduce the rodent stomach pH and facilitate nitration^{85,86}. In the context of NO₂-CLA formation during

inflammation, local administration of CLA as a free acid increased NO₂-CLA during peritoneal or vaginal inflammation³⁷. While these prior studies established that the necessary conditions to support nitration were present in vivo, they failed to support the typical formation under physiological and pathological conditions. In this work, we have established a mouse model to study endogenous lipid nitration reactions by using a dietary approach consisting of CLA-containing triglycerides. CLA was provided at the appropriate concentration and reached the right compartments to evaluate its metabolism and immunomodulatory effects, modeling human consumption where dietary CLA from dairy sources is primarily found esterified to triglycerides.

Before this study, NO₂-CLA was viewed as a delayed anti-inflammatory signaling lipid that needed to be formed by increased iNOS and •NO₂ formation, a process that peaks after 4-6 hours post stimulus^{37,63}. This paradigm of delayed synthesis was incompatible with the global anti-inflammatory effects reported for these compounds. Our data shows that preformed NO₂-CLA is present before iNOS induction, and in this context is an active early modulator of protective responses. In this regard, we found that membranes act as capacitors for NO₂-CLA by storing it in phospholipids, forming a pool that can be rapidly hydrolyzed by PLA2. The subsequent release of NO₂-CLA induces anti-inflammatory effects mediated by interfering with TLR4-dependent responses upstream of NF- κ B⁶⁶. Once depleted, the membrane nitroalkene levels need to be restored, which requires NO₂-CLA gastric synthesis and membrane remodeling by iterations of the Land's cycle. While previous acute models undoubtedly confirmed the nitration of CLA, our study shows the net loss of NO₂-CLA with consumption outweighing the de novo synthesis^{32,37}. Despite the significant levels of membrane-accumulated CLA, increased •NO formation and favorable nitration kinetics in membranes failed to compensate for the extensive hydrolysis of NO₂-CLA^{21,87}. This is likely due to the inability of parenchymal tissue to generate NO₂-CLA as efficiently as macrophages and cell types that have strong iNOS responses, thereby relying on the levels stored beforehand. Effectively, the mechanism provides an initial burst of NO₂-CLA that

was not anticipated by findings from previous models, emphasizing the value of the models developed in this study.

Considering that murine macrophages exhibit a significantly higher magnitude of iNOS responses to LPS and IFN γ compared to human macrophages and monocytes, the role of iNOS-dependent CLA nitration is likely to be even less prominent in humans, which we speculate further underscores the importance of preformed, diet-dependent NO₂-CLA in membranes. In fact, humans are significantly more adept at gastric lipid nitration by concentrating nitrite 20 \times in the saliva and preserving a more acidic stomach pH than mice⁸⁸. We monitored the depletion of NO₂-CLA in the plasma of septic shock patients (Fig. 8) and accumulation of released nitroalkene in urine (Fig. 6). Depending on the severity of sepsis or endotoxemia, these patients may have received enteral or parenteral nutrition, which lack conjugated fatty acids and bypasses the stomach (IV administration). Neither nutrient intake supports gastric NO₂-CLA synthesis, so membranes cannot be recharged with nitroalkene until resolution of the inflammatory crisis, highlighting the value of restoring the protective levels of NO₂-CLA.

There is a global redistribution of NO₂-CLA during inflammation, targeting tissues and different cell types. However, from these targets, the endothelium appears to be a critical that contributes to maintaining the vascular tone in CLA-treated mice after LPS challenge. Hypotension is a severe consequence of sepsis and reflects the dysregulated synthesis of •NO, where smooth muscle cells normally responsive to small •NO fluxes derived from eNOS (μ M) become overactivated with high local •NO levels derived from iNOS (mM)⁶³. CLA cannot directly quench •NO, and it is unlikely that sequestration of the autoxidation product •NO₂ would impact blood pressure regulation to such a significant extent. Thus, we view NO₂-CLA to mediate protection against severe vasorelaxation through reduced endothelial cell activation and reduced leakiness, preventing inflammatory cell permeation into the subendothelial space. The pharmacological agent 10-NO₂-OA inhibits TLR4 upregulation and NF- κ B adaptor protein

recruitment in endothelial cells, thereby mitigating pro-inflammatory signaling at an early stage⁶⁶. This mechanism may extend to endogenous NO₂-CLA.

CLA is a unique biological “sponge” for •NO₂, as not all biomolecules containing a conjugated diene participate in addition reactions and form a reactive nitroalkene. As an example, •NO₂ reacts with 7-dihydrocholesterol (7-DHC), polyunsaturated fatty acids, and tyrosine, by abstracting hydrogen instead of addition reactions, leading to oxidized products^{19,89}. Alternatively, the availability of CLA and its unusual chemical reactivity towards •NO₂ lends itself to the formation of NO₂-CLA while quenching the indiscriminate biomolecule oxidation induced by •NO₂. In this regard, the proclivity of CLA towards •NO₂ may play a protective role during acute and chronic pathologies, including cancer, atherosclerosis, sickle cell anemia, and metabolic disease, where oxidative stress and radical reactions induce tissue damage. The biological functions and health benefits of CLA have been evaluated in most of these contexts but work in the last decade has primarily focused on the anti-cancer properties of conjugated fatty acids^{12,90,91}. Alongside ferroptotic cell death induced by conjugated linolenic acid isomers, antineoplastic and chemosensitizing effects by NO₂-FAs have been reported⁹²⁻⁹⁴. While CLA itself has low toxicity in cancer cell lines compared to other conjugated fatty acids, the contributions of heightened •NO and enrichment of these conjugated dienes in tumor microenvironments may better promote synthesis of NO₂-CLA and achieve some of the pharmacological effects reported with exogenous nitroalkenes⁹⁵.

A major barrier in the field was to reconcile the timing and biological effects with the extent of CLA nitration and the analytical challenges. This work unifies these concepts, providing a new framework to evaluate the formation and role of lipid nitration and the modulation of the inflammatory processes by CLA.

Experimental Model and Study Participant Details

Human subjects

Human plasma samples from ICU patients and non-ICU controls were collected under an approved institutional review board (IRB) protocol at the University of Alabama at Birmingham (IRB-300005209). Urine samples from volunteer participants were collected under an approved IRB protocol at the University of Pennsylvania (IRB810598).

Animals

All animal procedures were approved by the University of Pittsburgh Institutional Animal Care and Use Committee (IACUC approval #23093600). Male C57BL/6J mice (8 weeks old) were obtained from Jackson Laboratory and maintained under standard housing conditions with a 12-hour light/dark cycle and ad libitum access to food and water. Mice were randomized into experimental groups (n = 8 per group) and fed either a control diet (AIN-93G; Research Diets, D10012G) or a 1% conjugated linoleic acid (CLA)-supplemented diet (Research Diets, D23022005) for 4 weeks.

Cell lines

RAW264.7 macrophages were cultured in complete Roswell Park Memorial Institute (RPMI) 1640 medium supplemented with 10% FBS and 100 U/ml penicillin/streptomycin at 37 °C in a humidified atmosphere containing 5% CO₂. Cells were treated with 50 µM of either CLA (Nature's Bounty) or linoleic acid (Nu-Check Prep, Inc.) in medium containing 2% FBS for 72 hours.

Method Details

Dietary CLA formulation

Allometric scaling was used to calculate the CLA dose for mouse dietary intervention studies. The average human consumption of CLA supplements is 3,000-4,000 mg/day, equating to 43-57 mg/kg/day for a 70 kg person. To meet the lower end of human supplementation, mice received a 1% CLA, allowing for 560 mg/kg/day based on an average food intake of 2.8 g/day and weight of 0.05 kg. Based on human intake (3–4 g/day; ~43–57 mg/kg/day), mice were administered a 1% CLA diet corresponding to ~560 mg/kg/day, assuming an average food intake of 2.8 g/day and body weight of 0.05 kg. This corresponds to a human equivalent dose of ~45.4 mg/kg/day. The CLA diet was prepared by replacing 1% of soybean oil in the AIN-93G formulation (Growing Rodent Diet, Research Diets, D10012G) with Tonalin CLA (BASF), accounting for 80% purity.

In vitro LPS challenge

For induction of NO₂-FA formation, CLA-supplemented RAW264.7 macrophages were stimulated with lipopolysaccharide (LPS) from *Escherichia coli* O111:B4 (100 ng/ml) and mouse IFN γ (200 for 24 hours. For IL-6 cytokine levels in the supernatant and mRNA levels, RAW264.7 cells were challenged with LPS for 6 hours.

In vivo LPS challenge and sample collection

Following 4 weeks of dietary intervention, mice were housed in metabolic cages for 24 hours to collect urine. Mice were then injected intraperitoneally with saline or sublethal dose of LPS (5

mg/kg). Endotoxemia was allowed to proceed for 6 or 16 hours. Mice were euthanized under isoflurane anesthesia, and blood was collected by venipuncture. Plasma was isolated by centrifugation ($10,000 \times g$, 5 min, 4°C). Tissues were harvested, snap-frozen in liquid nitrogen, and stored at -80°C .

Telemetry measurements

For blood pressure monitoring during in vivo LPS challenge, mice were implanted with telemetry devices (HDX-10, Data Sciences International) in the left common carotid artery under isoflurane anesthesia. Following a 14-day recovery period, baseline systolic blood pressure was recorded for 24 hours. LPS was administered intraperitoneally between 2–3 PM to control for circadian variation. Changes in systolic pressure were calculated relative to time-matched baseline measurements.

Lipid extraction and processing

Cell samples: For NO_2 -CLA measurements, cell pellets were extracted using ethyl acetate (500 μl) and water (200 μl) in the presence of 15 pmoles of $^{15}\text{NO}_2$ - $d_4\text{OA}$ and $^{15}\text{NO}_2$ - $d_4\text{SA}$ and 25 pmoles of heptadecanoic acid. Following centrifugation ($1,000 \times g$, 5 min, 4°C), the organic phase was collected and dried under nitrogen. For total fatty acid analysis, samples were subjected to base hydrolysis (1 M KOH in methanol, 60°C , 1 hour), neutralized with HCl, and re-extracted. For phospholipid-specific analysis of CLA, extracted cell pellets were resuspended in hexane, and lipid fractions were separated with Strata NH2 columns (see lipid fraction section). The phospholipid fraction was incubated in Tris-NaCl buffer (50 mM, pH 8.0) with Phospholipase A1 from *Aspergillus oryzae* or phospholipase A2 from porcine pancreas for 2 hours at 37°C . Samples were re-extracted with ethyl acetate and subject to PFB derivatization. For NO_2 -CLA-CoA detection, cells were precipitated directly in the plate with 80% methanol.

Plasma: Analysis of free (non-esterified) NO_2 -CLA, metabolites, and native fatty acids was performed by adding ethyl acetate (500 μl) and water (200 μl) to plasma (100 μl) in the presence of 15 pmoles of $^{15}\text{NO}_2$ - $d_4\text{OA}$ and $^{15}\text{NO}_2$ - $d_4\text{SA}$ and 25 pmoles of heptadecanoic acid as internal standards. Samples were vortexed, centrifuged at $1,000 \times g$ for 5 min at 4°C , and the upper phase transferred into a clean tube and dried under nitrogen. Samples were resuspended in 100 μl acetonitrile/ethyl acetate (80/20, v/v) for HPLC-MSMS analysis. To obtain the total NO_2 -FA content (free acid plus esterified), the extracted plasma was subjected to acid hydrolysis. Samples were incubated with acetonitrile (800 μl), water (100 μl), and fuming HCl (100 μl) at 90°C for 1 hour. After hydrolysis, NO_2 -FAs were re-extracted using ethyl acetate (1 ml). The solvent was dried under a stream of nitrogen, and NO_2 -FAs were reconstituted in acetonitrile (100 μl) for further analysis.

Urine: The urine samples (1 ml from mice and 200 μl from humans) were spiked with 15 pmoles of $^{15}\text{NO}_2$ - $d_4\text{OA}$ and $^{15}\text{NO}_2$ - $d_4\text{SA}$ as internal standards. The concentration of nitroalkene (free acid plus Michael adducts) was obtained by incubating the urine samples with 20 mM mercury (II) chloride (HgCl_2) for 30 min at 37°C before extraction. The Hg^{2+} competes for the nitroalkene-adducted cysteine, displacing the equilibrium with the elimination of the nitroalkene and formation of Hg-cysteine adducts. After that, urine samples were extracted using HyperSepTM C18 SPE

Cartridges (500 mg/3 ml). Columns were conditioned with 100% methanol, followed by 2 column volumes of 10% methanol. Samples were loaded and the SPE columns washed with 2 column volumes of 10% methanol and dried under vacuum for 30 min. Lipids were eluted with 3 ml methanol, the solvent evaporated under a stream of nitrogen, and samples reconstituted in 100 μ l of methanol for HPLC-MSMS analysis.

Tissue: Tissue samples were weighed and pulverized. Tissues were homogenized in water and extracted similarly to plasma. For thiol adduct analysis, elimination was performed using the same conditions as outlined for urine.

Lipid fractionation: Lipid classes were purified using solid phase extraction Strata NH₂ columns (500 mg/ 3ml). Columns were preconditioned by washing twice with 2 ml acetone/water (7:1, v/v) and twice with 2 ml hexane. The samples solubilized in hexane/methyl tert-butyl ether/acetic acid (100/3/0.3 v/v/v) were loaded on the columns and cholesterol esters (CEs), TGs, MAG+DAGs, FFAs, phospholipids were sequentially eluted with hexane, hexane/chloroform/ethyl acetate (100:5:5, v/v/v), chloroform/2-propanol (2:1, v/v), diethyl ether/2% acetic acid, methanol, respectively. The solvents were evaporated under a stream of nitrogen and then CEs and TGs were dissolved in ml ethyl acetate, while phospholipid fractions were solvated in 0.2 ml methanol. HPLC-CAD-MS analysis of each fraction confirmed lipid class composition. Standard curves prepared in each fraction's matrix were prepared to quantify the class abundance.

GC-MS Analysis of fatty acids

Lipid extracts in acetonitrile from cell culture and tissue were treated with 1% N-N-Diisopropylethylamine (100 μ l) and 2% PFB (100 μ l) (both solutions prepared in ACN) for 30 min at RT. Samples were dried under nitrogen and resuspended in 100 μ l ACN. Fatty acid-PFB esters from RAW264.7 macrophage pellets and tissue were analyzed using a Trace 1310 GC coupled to a TSQ9000 triple quadrupole mass spectrometer in negative chemical ionization mode (nCI). Samples (1 μ l) were injected in the splitless mode onto an Agilent DB-5 column (15m x 0.25mm x 0.25 μ m film thickness). The column was held at 60°C for 1 min, and then the temperature was increased to 280°C at a rate of 15°C/min. Helium and methane (1 ml/min) were used as the carrier and reagent gas, respectively. Scans were recorded for the m/z range 200-400. The corresponding MS filters for fatty acids are: 14:0 (m/z 227-227.5), 16:1 (m/z 253-253.5), 16:0 (m/z 255-255.5), CLA/18:2 (m/z 279-279.5), 18:1 (m/z 281-281.5), 20:4 (m/z 303-303.5), 20:3 (m/z 305-305.5), 20:2 (m/z 307-307.5), 20:1 (m/z 309-309.5), 20:0 (m/z 311-311.5), 22:6 (m/z 327-327.5), 22:5 (m/z 329-329.5). The sample injector and GC/MS transfer line were kept at 250°C and 280°C, respectively.

HPLC-MSMS analysis of NO₂-FAs

NO₂-FA lipid extracts were analyzed by HPLC-ESI-MSMS using gradient solvent systems consisting of water containing 0.1% acetic acid (solvent A) and acetonitrile containing 0.1% acetic acid (solvent B). Urine and tissue extracts were resolved for quantification and characterization using a reverse phase HPLC column (2 \times 100 mm 5 μ m Luna C18(2) column; Phenomenex) at a 0.65 ml/min flow rate. Samples were loaded onto the column at 35% B, maintained for 0.3 min, and eluted with a linear increase in solvent B from 35-100% of B over 8 min. The analysis was

performed using a QTRAP 6500+ triple quadrupole mass spectrometer in the negative ion mode. Source temperature was 600 °C, curtain gas: 40, ionization spray voltage: -4500, GS1: 55, GS2: 60. For collision induced fragmentations leading to either NO_2^- or $^{15}\text{NO}_2^-$ formation (m/z 46 and 47 respectively), the following settings were used: declustering potential: -80 V, entrance potential: -5 V, collision energy: -35 V and collision cell exit potential: -3 V. The corresponding MRM transitions are: $\text{NO}_2\text{-CLA}$ (324.2/46), $\text{red-NO}_2\text{-CLA}$ (326.2/46), $^{15}\text{NO}_2\text{-d}_4\text{OA}$ (331.2/47), and $^{15}\text{NO}_2\text{-d}_4\text{SA}$ (333.2/47). Transitions for β -oxidation metabolites were obtained by subtracting 28 amu from parent compounds and following collision-induced generation of 46 m/z ions as before. For characterization of $\text{NO}_2\text{-CLA}$, $\text{red-NO}_2\text{-CLA}$, and $\text{GSH-NO}_2\text{-CLA}$ in plasma, the same solvent system for urine and tissue was used with the following gradient: samples were loaded onto the column at 20% B, maintained for 0.3 min, and eluted with a linear increase in solvent B from 20-100% B over 14 minutes. The same MS settings were used. For collision-induced fragments leading to GSH formation (m/z 306), the following MS settings were used: declustering potential: -80 V, entrance potential: -5 V, collision energy: -25 V, and collision cell exit potential: -8 V. The MRM transition for $\text{NO}_2\text{-CLA-GSH}$ is 631.2/306.

HPLC-MSMS analysis of $\text{NO}_2\text{-CLA-CoA}$ adducts

$\text{NO}_2\text{-CLA-CoA}$ adducts in RAW264.7 macrophages were analyzed by HPLC-HR-MSMS using gradient solvent systems consisting of water containing 0.1% NH_4OH (solvent A) and acetonitrile containing 0.1% NH_4OH (solvent B). Samples were resolved for qualitative characterization using a reverse-phase HPLC column (2 × 150 mm, 5 μm Luna C8(2) column; Phenomenex) at a 0.5 ml/min flow rate. Samples were loaded onto the column at 5% B, maintained for 0.3 min and eluted with a linear increase in solvent B from 5-45% of B over 3 min then 45-65% B over 2 min. A Vanquish UPLC system connected to a Q-Exactive hybrid quadrupole-Orbitrap mass spectrometer was used in positive ion mode using the following parameters: sheath gas flow rate 40, aux gas flow rate 10, sweep gas flow rate 1.5, spray voltage 4kV, capillary temperature 325°C, S-lens RF level 50, aux gas heater temp 450°C. SIM for 1075.13-1075.56 at 35,000 resolution.

HPLC-MSMS analysis of nitrated phospholipids

Nitrated phospholipids in RAW264.7 macrophages were analyzed by HPLC-HR-MSMS using gradient solvent systems consisting of water/acetonitrile (50/50, v/v) containing 0.2% ammonium formate (solvent A) and isopropanol/acetonitrile/water (95/4.9/0.1, v/v/v) containing 0.1% ammonium formate (solvent B). Samples were resolved for qualitative characterization using a reverse-phase HPLC column (2 × 150 mm, 5 μm Luna C8(2) column; Phenomenex) at a 0.45 ml/min flow rate. Samples were loaded onto the column at 10% B, maintained for 0.3 min and eluted with a linear increase in solvent B from 10-100% of B over 7 min. The analysis was carried out using a Vanquish UHPLC system coupled to a Q-Exactive hybrid quadrupole-Orbitrap mass spectrometer in positive ion mode using the following parameters: sheath gas flow rate 56, aux gas flow rate 16, sweep gas flow rate 3, spray voltage 3.5kV, capillary temperature 300°C, S-lens RF level 75, aux gas heater temp 450°C. Full mass scan ranged from 400-1000 m/z at 35,000 resolution. Data-dependent top 5 masses were selected for MS2 fragmentation.

Plasma Cytokine Multiplex and ELISA

Plasma cytokines were quantified using the MILLIPLEX® Mouse Cytokine/Chemokine Magnetic Bead Panel Assay following the manufacturer's instructions. IL-6 levels in the RAW264.7 macrophage supernatants were quantified using the BD OptEIA™ Mouse IL-6 ELISA Kit following the manufacturer's instructions.

Quantitative PCR (qPCR)

Total RNA was extracted using TRIzol® Reagent (Invitrogen), according to the manufacturer's instructions. One microgram of RNA was reverse transcribed in a total volume of 20 µl using the iScript™ cDNA Synthesis Kit (Bio-Rad). Quantitative PCR was performed using TaqMan™ Fast Advanced Master Mix (Applied Biosystems) and TaqMan™ Gene Expression Assays for IL-1β and IL-6. Reactions were run on a QuantStudio™ 5 Real-Time PCR System (384-well block; Applied Biosystems) using the following cycling conditions: initial denaturation at 95 °C for 20 s, followed by 40 cycles of 95 °C for 1 s and 60°C for 20 s. Each sample was analyzed in triplicate. No amplification was observed in no-template controls (diethylpyrocarbonate-treated water) or in reverse transcription-negative controls.

Quantification and statistical analysis

Quantification of NO₂-CLA and metabolites was conducted in multiple reaction monitoring (MRM) mode using a QTRAP 6500+ triple quadrupole mass spectrometer. Calibration curves were generated using synthetic NO₂-CLA, ¹⁵NO₂-d₄OA and ¹⁵NO₂-d₄SA to quantify NO₂-CLA and its β-oxidation products. NO₂-FA levels in urine were normalized to urinary creatinine, which was measured using a colorimetric assay kit based on absorbance at 500 nm. All statistical analysis was performed using GraphPad Prism software and indicated in the figure legends. Each experiment (>3 replicates within each experiment) was performed at least three independent times.

Key Resources Table

REAGENT or RESOURCE	SOURCE	IDENTIFIER
Antibodies		
N/A		
Bacterial and virus strains		
N/A		
Biological samples		
Endotoxemia human urine	University of Pennsylvania	IRB-810598
ICU and non-ICU human plasma	University of Alabama at Birmingham	IRB-300005209
Chemicals, peptides, and recombinant proteins		
Lipopolysaccharide (<i>Escherichia coli</i> O111:B4)	Sigma-Aldrich	Cat# L3024
Mouse IFN gamma, Recombinant Protein	Invitrogen	Cat # PIRP8617
1400W iNOS Inhibitor	Cayman Chemical	Cat# 81520
Phospholipase A1 (<i>Aspergillus oryzae</i>)	Sigma-Aldrich	Cat# L3295-50ML
Phospholipase A2 from porcine pancreas	Sigma-Aldrich	Cat# P6534

Heptadecanoic acid (C17:0)	Sigma-Aldrich	Cat# H3500
Pentafluorobenzyl bromide	Sigma-Aldrich	Cat#90257
N,N-diisopropylethylamine	Sigma-Aldrich	Cat# 387649
Conjugated linoleic acid (Tonalin TG 80)	BASF	PRD-No. 30531865
Conjugated linoleic acid	Nature's Bounty	https://naturesbounty.com/products/cila-1000-mg-50-rapid-release-softgels
Linoleic acid	Nu-Chek	Cat# U-59-A
¹⁵ NO ₂ -d ₄ -OA and ¹⁵ NO ₂ -d ₄ -SA internal standards	Woodcock et.al ⁵²	N/A
TRIzol™ Reagent	Invitrogen	Cat# 15596026
iScript™ cDNA Synthesis Kit	Bio-Rad	Cat# 1708891
TaqMan™ Fast Advanced Master Mix	Applied Biosystems	Cat# 4444557
Critical commercial assays		
BD OptEIA™ Mouse IL-6 ELISA Kit	BD Biosciences	Cat# BDB550950
MILLIPLEX® Mouse Cytokine/Chemokine Magnetic Bead Panel Assay	Millipore	Cat# MCYTOMAG-70K
Creatinine (urinary) Colorimetric Assay Kit	Cayman Chemical	Cat# 500701
Deposited data		
N/A		
Experimental models: Cell lines		
Mouse: RAW264.7	ATCC	ATCC TIB-71
Experimental models: Organisms/strains		
Mouse: C57BL6J	The Jackson Laboratory	RRID:IMSR_JAX:000664
Oligonucleotides		
TaqMan Gene Expression Assay (Mouse IL-6)	Applied Biosystems	Mm00446190_m1
TaqMan Gene Expression Assay (Mouse IL-1β)	Applied Biosystems	Mm00434228_m1
Recombinant DNA		
N/A		
Software and algorithms		
GraphPad Prism 10.6	GraphPad	https://www.graphpad.com/
Analyst 1.6.3	SCIEX	https://sciex.com/products/software/analyst-software
Chromeleon 7.3	Thermo Scientific	https://www.thermo.com/order/catalog/product/CHROMELEON7
Xcalibur 4.3	Thermo Scientific	https://www.thermo.com/order/catalog/product/OPTON-30965
LIPID MAPS® Structure Database (LMSD)	LIPID MAPS	https://www.lipidmaps.org/resources/tools/bulk-

		structure-search/create?database=LMSD
Other		
TSQ9000 Triple Quadrupole MS	Thermo Scientific	https://www.thermo.com/order/catalog/product/TSQ90BOP
6500+ QTRAP Triple Quadrupole MS	SCIEX	https://sciex.com/products/mass-spectrometers/triple-quad-systems/triple-quad-6500plus-system
Q Exactive Orbitrap MS	Thermo Scientific	https://www.thermo.com/us/en/home/industrial/mass-spectrometry/liquid-chromatography-mass-spectrometry-lc-ms.html
Vanquish HPLC-CAD	Thermo Scientific	https://www.thermo.com/us/en/home/industrial/chromatography/liquid-chromatography-lc/hplc-uhplc-systems.html
Strata NH2 (55 μ m, 70 Å), 500 mg / 3 mL, Tubes	Phenomenex	Part: 8B-S009-HBJ
HyperSep™ C18 Cartridges, 500 mg / 3mL	Thermo Scientific	Cat# 60108-304

Acknowledgments

We would like to thank Dr. Luis Villacorta for valuable discussion. Work performed in the UPMC Cancer Proteomics Facility: Luminex Core Laboratory and services and instruments used in this project were graciously supported, in part, by the University of Pittsburgh. This work was supported by National Institutes of Health (NIH) grants: 1F31 HL172595 and 5T32GM133332 (NC); R01 GM125944 and R01AR084311 (FJS); R35GM152083 and R01AI178864 (DAV); R01HL153113 (AG and RPP); R35HL161177 (ACS); **R01HD115342 (LV)**.

Author Contributions

NC Conceptualization, project management, investigation, methodology, formal analysis, writing original draft and reviewing, funding acquisition. **SRS, MMV** Investigation and formal analysis. **MVG, SH, KR** Investigation and methodology. **MB, AS** Methodology. **LV Resources & formal analysis**. **DAV** Review & editing. **CS, RPP, FV, AG, ACS** Resources, review & editing. **FJS** Conceptualization, formal analysis, writing and editing, funding acquisition. All authors have read and agreed to the published version of the manuscript.

Declaration of Interests

FJS declares financial interest in Creegh Pharmaceuticals Inc. and Furanica Inc. ACS is a consultant and stockholder for Creegh Pharmaceuticals. ACS received research funds from Bayer Pharmaceuticals. AG is stockholder of Alveolus Bio and Resbiotic. All other authors declare that they have no conflicts of interest with the contents of this article.

Bibliography

- 1 Qi, H. Y. & Shelhamer, J. H. Toll-like receptor 4 signaling regulates cytosolic phospholipase A2 activation and lipid generation in lipopolysaccharide-stimulated macrophages. *J Biol Chem* **280**, 38969-38975, doi:10.1074/jbc.M509352200 (2005).
- 2 Amunugama, K., Pike, D. P. & Ford, D. A. The lipid biology of sepsis. *J Lipid Res* **62**, 100090, doi:10.1016/j.jlr.2021.100090 (2021).
- 3 Hajeyah, A. A., Griffiths, W. J., Wang, Y., Finch, A. J. & O'Donnell, V. B. The Biosynthesis of Enzymatically Oxidized Lipids. *Front Endocrinol (Lausanne)* **11**, 591819, doi:10.3389/fendo.2020.591819 (2020).
- 4 Talukdar, S., Olefsky, J. M. & Osborn, O. Targeting GPR120 and other fatty acid-sensing GPCRs ameliorates insulin resistance and inflammatory diseases. *Trends Pharmacol Sci* **32**, 543-550, doi:10.1016/j.tips.2011.04.004 (2011).
- 5 Schopfer, F. J., Cipollina, C. & Freeman, B. A. Formation and signaling actions of electrophilic lipids. *Chem Rev* **111**, 5997-6021, doi:10.1021/cr200131e (2011).
- 6 Schopfer, F. J. *et al.* Detection and quantification of protein adduction by electrophilic fatty acids: mitochondrial generation of fatty acid nitroalkene derivatives. *Free Radic Biol Med* **46**, 1250-1259, doi:10.1016/j.freeradbiomed.2008.12.025 (2009).
- 7 Beavers, W. N. *et al.* Protein Modification by Endogenously Generated Lipid Electrophiles: Mitochondria as the Source and Target. *ACS Chem Biol* **12**, 2062-2069, doi:10.1021/acscchembio.7b00480 (2017).
- 8 Chen, Y. *et al.* Chemoproteomic profiling of targets of lipid-derived electrophiles by bioorthogonal aminoxy probe. *Redox Biol* **12**, 712-718, doi:10.1016/j.redox.2017.04.001 (2017).
- 9 Fang, M. Y. *et al.* Chemoproteomic profiling reveals cellular targets of nitro-fatty acids. *Redox Biol* **46**, 102126, doi:10.1016/j.redox.2021.102126 (2021).
- 10 Do, Q. *et al.* Development and Application of a Peroxyl Radical Clock Approach for Measuring Both Hydrogen-Atom Transfer and Peroxyl Radical Addition Rate Constants. *J Org Chem* **86**, 153-168, doi:10.1021/acs.joc.0c01920 (2021).
- 11 Do, Q., Zhang, R., Hooper, G. & Xu, L. Differential Contributions of Distinct Free Radical Peroxidation Mechanisms to the Induction of Ferroptosis. *JACS Au* **3**, 1100-1117, doi:10.1021/jacsau.2c00681 (2023).
- 12 Beatty, A. *et al.* Ferroptotic cell death triggered by conjugated linolenic acids is mediated by ACSL1. *Nat Commun* **12**, 2244, doi:10.1038/s41467-021-22471-y (2021).
- 13 Colussi N, C. F., Schopfer FJ. The specificity of endogenous fatty acid nitration: only conjugated substrates support the in vivo formation of nitro-fatty acids. *Redox Biochem Chem* **9**, doi:10.1016/j.rbc.2024.100037. (2024).
- 14 Bonacci, G. *et al.* Conjugated linoleic acid is a preferential substrate for fatty acid nitration. *J Biol Chem* **287**, 44071-44082, doi:10.1074/jbc.M112.401356 (2012).
- 15 Woodcock, S. R., Salvatore, S. R., Bonacci, G., Schopfer, F. J. & Freeman, B. A. Biomimetic nitration of conjugated linoleic acid: formation and characterization of naturally occurring conjugated nitrodienes. *J Org Chem* **79**, 25-33, doi:10.1021/jo4021562 (2014).
- 16 Pryor, W. A. & Lightsey, J. W. Mechanisms of nitrogen dioxide reactions: initiation of lipid peroxidation and the production of nitrous Acid. *Science* **214**, 435-437, doi:10.1126/science.214.4519.435 (1981).
- 17 Gallon, A. A. & Pryor, W. A. The identification of the allylic nitrite and nitro derivatives of methyl linoleate and methyl linolenate by negative chemical ionization mass spectroscopy. *Lipids* **28**, 125-133, doi:10.1007/bf02535776 (1993).

- 18 Gallon, A. A. & Pryor, W. A. The reaction of low levels of nitrogen dioxide with methyl linoleate in the presence and absence of oxygen. *Lipids* **29**, 171-176, doi:10.1007/bf02536725 (1994).
- 19 Jiang, H. *et al.* Nitrogen dioxide induces cis-trans-isomerization of arachidonic acid within cellular phospholipids. Detection of trans-arachidonic acids in vivo. *J Biol Chem* **274**, 16235-16241, doi:10.1074/jbc.274.23.16235 (1999).
- 20 Möller, M. N. & Vitturi, D. A. The chemical biology of dinitrogen trioxide. *Redox Biochem Chem* **8**, doi:10.1016/j.rbc.2024.100026 (2024).
- 21 Möller, M. N. *et al.* Membrane "lens" effect: focusing the formation of reactive nitrogen oxides from the *NO/O₂ reaction. *Chem Res Toxicol* **20**, 709-714, doi:10.1021/tx700010h (2007).
- 22 Rudolph, V. *et al.* Endogenous generation and protective effects of nitro-fatty acids in a murine model of focal cardiac ischaemia and reperfusion. *Cardiovasc Res* **85**, 155-166, doi:10.1093/cvr/cvp275 (2010).
- 23 Ecker, J., Liebisch, G., Scherer, M. & Schmitz, G. Differential effects of conjugated linoleic acid isomers on macrophage glycerophospholipid metabolism. *J Lipid Res* **51**, 2686-2694, doi:10.1194/jlr.M007906 (2010).
- 24 Devillard, E., McIntosh, F. M., Duncan, S. H. & Wallace, R. J. Metabolism of linoleic acid by human gut bacteria: different routes for biosynthesis of conjugated linoleic acid. *J Bacteriol* **189**, 2566-2570, doi:10.1128/JB.01359-06 (2007).
- 25 Salsinha, A. S., Pimentel, L. L., Fontes, A. L., Gomes, A. M. & Rodríguez-Alcalá, L. M. Microbial Production of Conjugated Linoleic Acid and Conjugated Linolenic Acid Relies on a Multienzymatic System. *Microbiol Mol Biol Rev* **82**, doi:10.1128/mmbr.00019-18 (2018).
- 26 Song, X. *et al.* Gut microbial fatty acid isomerization modulates intraepithelial T cells. *Nature* **619**, 837-843, doi:10.1038/s41586-023-06265-4 (2023).
- 27 Salvatore, S. R., Rowart, P. & Schopfer, F. J. Mass spectrometry-based study defines the human urine nitrolipidome. *Free Radic Biol Med* **162**, 327-337, doi:10.1016/j.freeradbiomed.2020.10.305 (2021).
- 28 Baker, P. R., Schopfer, F. J., O'Donnell, V. B. & Freeman, B. A. Convergence of nitric oxide and lipid signaling: anti-inflammatory nitro-fatty acids. *Free Radic Biol Med* **46**, 989-1003, doi:10.1016/j.freeradbiomed.2008.11.021 (2009).
- 29 Freeman, B. A. *et al.* Nitro-fatty acid formation and signaling. *J Biol Chem* **283**, 15515-15519, doi:10.1074/jbc.R800004200 (2008).
- 30 Turell, L., Steglich, M. & Alvarez, B. The chemical foundations of nitroalkene fatty acid signaling through addition reactions with thiols. *Nitric Oxide*, doi:10.1016/j.niox.2018.03.014 (2018).
- 31 Cui, T. *et al.* Nitrated fatty acids: Endogenous anti-inflammatory signaling mediators. *J Biol Chem* **281**, 35686-35698, doi:10.1074/jbc.M603357200 (2006).
- 32 Hansen, A. L. *et al.* Nitro-fatty acids are formed in response to virus infection and are potent inhibitors of STING palmitoylation and signaling. *Proc Natl Acad Sci U S A* **115**, E7768-e7775, doi:10.1073/pnas.1806239115 (2018).
- 33 Bago, A. *et al.* Nitro-oleic acid regulates T cell activation through post-translational modification of calcineurin. *Proc Natl Acad Sci U S A* **120**, e2208924120, doi:10.1073/pnas.2208924120 (2023).
- 34 Wang, P. *et al.* Electrophilic nitro-fatty acids suppress psoriasiform dermatitis: STAT3 inhibition as a contributory mechanism. *Redox Biol* **43**, 101987, doi:10.1016/j.redox.2021.101987 (2021).
- 35 Villacorta, L. *et al.* Nitro-linoleic acid inhibits vascular smooth muscle cell proliferation via the Keap1/Nrf2 signaling pathway. *Am J Physiol Heart Circ Physiol* **293**, H770-776, doi:10.1152/ajpheart.00261.2007 (2007).

- 36 Kansanen, E. *et al.* Nrf2-dependent and -independent responses to nitro-fatty acids in human endothelial cells: identification of heat shock response as the major pathway activated by nitro-oleic acid. *J Biol Chem* **284**, 33233-33241, doi:10.1074/jbc.M109.064873 (2009).
- 37 Villacorta, L. *et al.* In situ generation, metabolism and immunomodulatory signaling actions of nitro-conjugated linoleic acid in a murine model of inflammation. *Redox Biol* **15**, 522-531, doi:10.1016/j.redox.2018.01.005 (2018).
- 38 Salvatore, S. R. *et al.* Characterization and quantification of endogenous fatty acid nitroalkene metabolites in human urine. *J Lipid Res* **54**, 1998-2009, doi:10.1194/jlr.M037804 (2013).
- 39 Obsen, T. *et al.* Trans-10, cis-12 conjugated linoleic acid decreases de novo lipid synthesis in human adipocytes. *J Nutr Biochem* **23**, 580-590, doi:10.1016/j.jnutbio.2011.02.014 (2012).
- 40 Choi, Y., Park, Y., Storkson, J. M., Pariza, M. W. & Ntambi, J. M. Inhibition of stearyl-CoA desaturase activity by the cis-9,trans-11 isomer and the trans-10,cis-12 isomer of conjugated linoleic acid in MDA-MB-231 and MCF-7 human breast cancer cells. *Biochem Biophys Res Commun* **294**, 785-790, doi:10.1016/s0006-291x(02)00554-5 (2002).
- 41 Subbaiah, P. V., Gould, I. G., Lal, S. & Aizezi, B. Incorporation profiles of conjugated linoleic acid isomers in cell membranes and their positional distribution in phospholipids. *Biochim Biophys Acta* **1811**, 17-24, doi:10.1016/j.bbalip.2010.09.004 (2011).
- 42 Park, Y. *et al.* Effect of conjugated linoleic acid on body composition in mice. *Lipids* **32**, 853-858, doi:10.1007/s11745-997-0109-x (1997).
- 43 den Hartigh, L. J. *et al.* Metabolically distinct weight loss by 10,12 CLA and caloric restriction highlight the importance of subcutaneous white adipose tissue for glucose homeostasis in mice. *PLoS One* **12**, e0172912, doi:10.1371/journal.pone.0172912 (2017).
- 44 Vyas, D., Kadegowda, A. K. & Erdman, R. A. Dietary conjugated linoleic Acid and hepatic steatosis: species-specific effects on liver and adipose lipid metabolism and gene expression. *J Nutr Metab* **2012**, 932928, doi:10.1155/2012/932928 (2012).
- 45 Kelley, D. S. *et al.* Contrasting effects of t10,c12- and c9,t11-conjugated linoleic acid isomers on the fatty acid profiles of mouse liver lipids. *Lipids* **39**, 135-141, doi:10.1007/s11745-004-1211-9 (2004).
- 46 Burdge, G. C. *et al.* Incorporation of cis-9,trans-11 or trans-10,cis-12 conjugated linoleic acid into plasma and cellular lipids in healthy men. *J Lipid Res* **45**, 736-741, doi:10.1194/jlr.M300447-JLR200 (2004).
- 47 Petridou, A., Mougios, V. & Sagredos, A. Supplementation with CLA: isomer incorporation into serum lipids and effect on body fat of women. *Lipids* **38**, 805-811, doi:10.1007/s11745-003-1129-2 (2003).
- 48 Schopfer, F. J. *et al.* Fatty acid nitroalkenes regulate intestinal lipid absorption. *J Lipid Res* **66**, 100855, doi:10.1016/j.jlr.2025.100855 (2025).
- 49 Vitturi, D. A. *et al.* Modulation of nitro-fatty acid signaling: prostaglandin reductase-1 is a nitroalkene reductase. *J Biol Chem* **288**, 25626-25637, doi:10.1074/jbc.M113.486282 (2013).
- 50 Steglich, M. *et al.* Human glutathione transferases catalyze the reaction between glutathione and nitrooleic acid. *J Biol Chem* **301**, 108362, doi:10.1016/j.jbc.2025.108362 (2025).
- 51 Turell, L. *et al.* The Chemical Basis of Thiol Addition to Nitro-conjugated Linoleic Acid, a Protective Cell-signaling Lipid. *J Biol Chem* **292**, 1145-1159, doi:10.1074/jbc.M116.756288 (2017).

- 52 Woodcock, S. R., Bonacci, G., Gelhaus, S. L. & Schopfer, F. J. Nitrated fatty acids: synthesis and measurement. *Free Radic Biol Med* **59**, 14-26, doi:10.1016/j.freeradbiomed.2012.11.015 (2013).
- 53 Delmastro-Greenwood, M. *et al.* Nitrite and nitrate-dependent generation of anti-inflammatory fatty acid nitroalkenes. *Free Radic Biol Med* **89**, 333-341, doi:10.1016/j.freeradbiomed.2015.07.149 (2015).
- 54 Garner, R. M., Mould, D. R., Chieffo, C. & Jorkasky, D. K. Pharmacokinetic and Pharmacodynamic Effects of Oral CXA-10, a Nitro Fatty Acid, After Single and Multiple Ascending Doses in Healthy and Obese Subjects. *Clin Transl Sci* **12**, 667-676, doi:10.1111/cts.12672 (2019).
- 55 Buchan, G. J., Bonacci, G., Fazzari, M., Salvatore, S. R. & Gelhaus Wendell, S. Nitro-fatty acid formation and metabolism. *Nitric Oxide* **79**, 38-44, doi:10.1016/j.niox.2018.07.003 (2018).
- 56 Grippo, V. *et al.* Electrophilic characteristics and aqueous behavior of fatty acid nitroalkenes. *Redox Biol* **38**, 101756, doi:10.1016/j.redox.2020.101756 (2021).
- 57 O'Donnell, V. B. New appreciation for an old pathway: the Lands Cycle moves into new arenas in health and disease. *Biochem Soc Trans* **50**, 1-11, doi:10.1042/BST20210579 (2022).
- 58 Misheva, M. *et al.* Oxylin metabolism is controlled by mitochondrial beta-oxidation during bacterial inflammation. *Nat Commun* **13**, 139, doi:10.1038/s41467-021-27766-8 (2022).
- 59 Neves, B. *et al.* Advancing Target Identification of Nitrated Phospholipids in Biological Systems by HCD Specific Fragmentation Fingerprinting in Orbitrap Platforms. *Molecules* **25**, doi:10.3390/molecules25092120 (2020).
- 60 Melo, T. *et al.* Characterization of phospholipid nitroxidation by LC-MS in biomimetic models and in H9c2 Myoblast using a lipidomic approach. *Free Radic Biol Med* **106**, 219-227, doi:10.1016/j.freeradbiomed.2017.02.033 (2017).
- 61 Montero-Bullon, J. F., Melo, T., Rosário, M. D. M. & Domingues, P. Liquid chromatography/tandem mass spectrometry characterization of nitroso, nitrated and nitroxidized cardiolipin products. *Free Radic Biol Med* **144**, 183-191, doi:10.1016/j.freeradbiomed.2019.05.009 (2019).
- 62 Melo, T. *et al.* Recent Advances on Mass Spectrometry Analysis of Nitrated Phospholipids. *Anal Chem* **88**, 2622-2629, doi:10.1021/acs.analchem.5b03407 (2016).
- 63 Palmieri, E. M., McGinity, C., Wink, D. A. & McVicar, D. W. Nitric Oxide in Macrophage Immunometabolism: Hiding in Plain Sight. *Metabolites* **10**, doi:10.3390/metabo10110429 (2020).
- 64 Turell, L. *et al.* The Chemical Basis of Thiol Addition to Nitro-conjugated Linoleic Acid, a Protective Cell-signaling Lipid. *J Biol Chem* **292**, 1145-1159, doi:10.1074/jbc.M116.756288 (2017).
- 65 Yang, T. *et al.* Inorganic nitrite attenuates NADPH oxidase-derived superoxide generation in activated macrophages via a nitric oxide-dependent mechanism. *Free Radic Biol Med* **83**, 159-166, doi:10.1016/j.freeradbiomed.2015.02.016 (2015).
- 66 Villacorta, L. *et al.* Electrophilic nitro-fatty acids inhibit vascular inflammation by disrupting LPS-dependent TLR4 signalling in lipid rafts. *Cardiovasc Res* **98**, 116-124, doi:10.1093/cvr/cvt002 (2013).
- 67 Kubala, L. *et al.* Modulation of arachidonic and linoleic acid metabolites in myeloperoxidase-deficient mice during acute inflammation. *Free Radic Biol Med* **48**, 1311-1320, doi:10.1016/j.freeradbiomed.2010.02.010 (2010).
- 68 Willenberg, I. *et al.* Characterization of changes in plasma and tissue oxylin levels in LPS and CLP induced murine sepsis. *Inflamm Res* **65**, 133-142, doi:10.1007/s00011-015-0897-7 (2016).

- 69 Gómez, C. *et al.* Quantitative metabolic profiling of urinary eicosanoids for clinical phenotyping. *J Lipid Res* **60**, 1164-1173, doi:10.1194/jlr.D090571 (2019).
- 70 Ferguson, J. F. *et al.* Omega-3 PUFA supplementation and the response to evoked endotoxemia in healthy volunteers. *Mol Nutr Food Res* **58**, 601-613, doi:10.1002/mnfr.201300368 (2014).
- 71 Salvatore, S. R., Vitturi, D. A., Fazzari, M., Jorkasky, D. K. & Schopfer, F. J. Evaluation of 10-Nitro Oleic Acid Bio-Elimination in Rats and Humans. *Sci Rep* **7**, 39900, doi:10.1038/srep39900 (2017).
- 72 Seemann, S., Zohles, F. & Lupp, A. Comprehensive comparison of three different animal models for systemic inflammation. *J Biomed Sci* **24**, 60, doi:10.1186/s12929-017-0370-8 (2017).
- 73 Carreño, M. *et al.* Nitrated fatty acids protect against acute kidney injury in sickle cell disease. *Blood Adv* **9**, 2886-2890, doi:10.1182/bloodadvances.2024015038 (2025).
- 74 Belury, M. A. & Harris, W. S. Omega-6 fatty acids, inflammation and cardiometabolic health: Overview of supplementary issue. *Prostaglandins Leukot Essent Fatty Acids* **139**, 1-2, doi:10.1016/j.plefa.2018.10.006 (2018).
- 75 Bonilla, D. L., Ly, L. H., Fan, Y. Y., Chapkin, R. S. & McMurray, D. N. Incorporation of a dietary omega 3 fatty acid impairs murine macrophage responses to Mycobacterium tuberculosis. *PLoS One* **5**, e10878, doi:10.1371/journal.pone.0010878 (2010).
- 76 Fang, X. *et al.* Omega-3 PUFA attenuate mice myocardial infarction injury by emerging a protective eicosanoid pattern. *Prostaglandins Other Lipid Mediat* **139**, 1-9, doi:10.1016/j.prostaglandins.2018.09.002 (2018).
- 77 Borniquel, S., Jadert, C. & Lundberg, J. O. Dietary conjugated linoleic acid activates PPARgamma and the intestinal trefoil factor in SW480 cells and mice with dextran sulfate sodium-induced colitis. *J Nutr* **142**, 2135-2140, doi:10.3945/jn.112.163931 (2012).
- 78 Bassaganya-Riera, J. & Hontecillas, R. Dietary conjugated linoleic acid and n-3 polyunsaturated fatty acids in inflammatory bowel disease. *Curr Opin Clin Nutr Metab Care* **13**, 569-573, doi:10.1097/MCO.0b013e32833b648e (2010).
- 79 Churrua, I., Fernández-Quintela, A. & Portillo, M. P. Conjugated linoleic acid isomers: differences in metabolism and biological effects. *Biofactors* **35**, 105-111, doi:10.1002/biof.13 (2009).
- 80 den Hartigh, L. J. Conjugated Linoleic Acid Effects on Cancer, Obesity, and Atherosclerosis: A Review of Pre-Clinical and Human Trials with Current Perspectives. *Nutrients* **11**, doi:10.3390/nu11020370 (2019).
- 81 Haghighatdoost, F. & Nobakht, M. G. B. F. Effect of conjugated linoleic acid on blood inflammatory markers: a systematic review and meta-analysis on randomized controlled trials. *Eur J Clin Nutr* **72**, 1071-1082, doi:10.1038/s41430-017-0048-z (2018).
- 82 Kamlage, B., Hartmann, L., Gruhl, B. & Blaut, M. Intestinal microorganisms do not supply associated gnotobiotic rats with conjugated linoleic acid. *J Nutr* **129**, 2212-2217, doi:10.1093/jn/129.12.2212 (1999).
- 83 Hughan, K. S. *et al.* Conjugated Linoleic Acid Modulates Clinical Responses to Oral Nitrite and Nitrate. *Hypertension* **70**, 634-644, doi:10.1161/HYPERTENSIONAHA.117.09016 (2017).
- 84 McConnell, E. L., Basit, A. W. & Murdan, S. Measurements of rat and mouse gastrointestinal pH, fluid and lymphoid tissue, and implications for in-vivo experiments. *J Pharm Pharmacol* **60**, 63-70, doi:10.1211/jpp.60.1.0008 (2008).
- 85 Fazzari, M. *et al.* Endogenous generation of nitro-fatty acid hybrids having dual nitrate ester (RONO(2)) and nitroalkene (RNO(2)) substituents. *Redox Biol* **41**, 101913, doi:10.1016/j.redox.2021.101913 (2021).

- 86 Salvatore, S. R. *et al.* Digestive interaction between dietary nitrite and dairy products generates novel nitrated linolenic acid products. *Food Chem* **437**, 137767, doi:10.1016/j.foodchem.2023.137767 (2024).
- 87 Sharma, J. N., Al-Omran, A. & Parvathy, S. S. Role of nitric oxide in inflammatory diseases. *Inflammopharmacology* **15**, 252-259, doi:10.1007/s10787-007-0013-x (2007).
- 88 Montenegro, M. F. *et al.* Profound differences between humans and rodents in the ability to concentrate salivary nitrate: Implications for translational research. *Redox Biol* **10**, 206-210, doi:10.1016/j.redox.2016.10.011 (2016).
- 89 Radi, R. Nitric oxide, oxidants, and protein tyrosine nitration. *Proc Natl Acad Sci U S A* **101**, 4003-4008, doi:10.1073/pnas.0307446101 (2004).
- 90 Dhar Dubey, K. K., Sharma, G. & Kumar, A. Conjugated Linolenic Acids: Implication in Cancer. *J Agric Food Chem* **67**, 6091-6101, doi:10.1021/acs.jafc.9b01379 (2019).
- 91 Basak, S. & Duttaroy, A. K. Conjugated Linoleic Acid and Its Beneficial Effects in Obesity, Cardiovascular Disease, and Cancer. *Nutrients* **12**, doi:10.3390/nu12071913 (2020).
- 92 Roos, J. *et al.* Nitro-fatty acids: promising agents for the development of new cancer therapeutics. *Trends Pharmacol Sci* **45**, 1061-1080, doi:10.1016/j.tips.2024.09.009 (2024).
- 93 Hong, L. *et al.* Small molecule nitroalkenes inhibit RAD51-mediated homologous recombination and amplify triple-negative breast cancer cell killing by DNA-directed therapies. *Redox Biol* **66**, 102856, doi:10.1016/j.redox.2023.102856 (2023).
- 94 Jelinska, M., Bialek, A., Gielecinska, I., Mojska, H. & Tokarz, A. Impact of conjugated linoleic acid administered to rats prior and after carcinogenic agent on arachidonic and linoleic acid metabolites in serum and tumors. *Prostaglandins Leukot Essent Fatty Acids* **126**, 1-8, doi:10.1016/j.plefa.2017.08.013 (2017).
- 95 McGinity, C. L. *et al.* Nitric Oxide Modulates Metabolic Processes in the Tumor Immune Microenvironment. *Int J Mol Sci* **22**, doi:10.3390/ijms22137068 (2021).

FIGURES

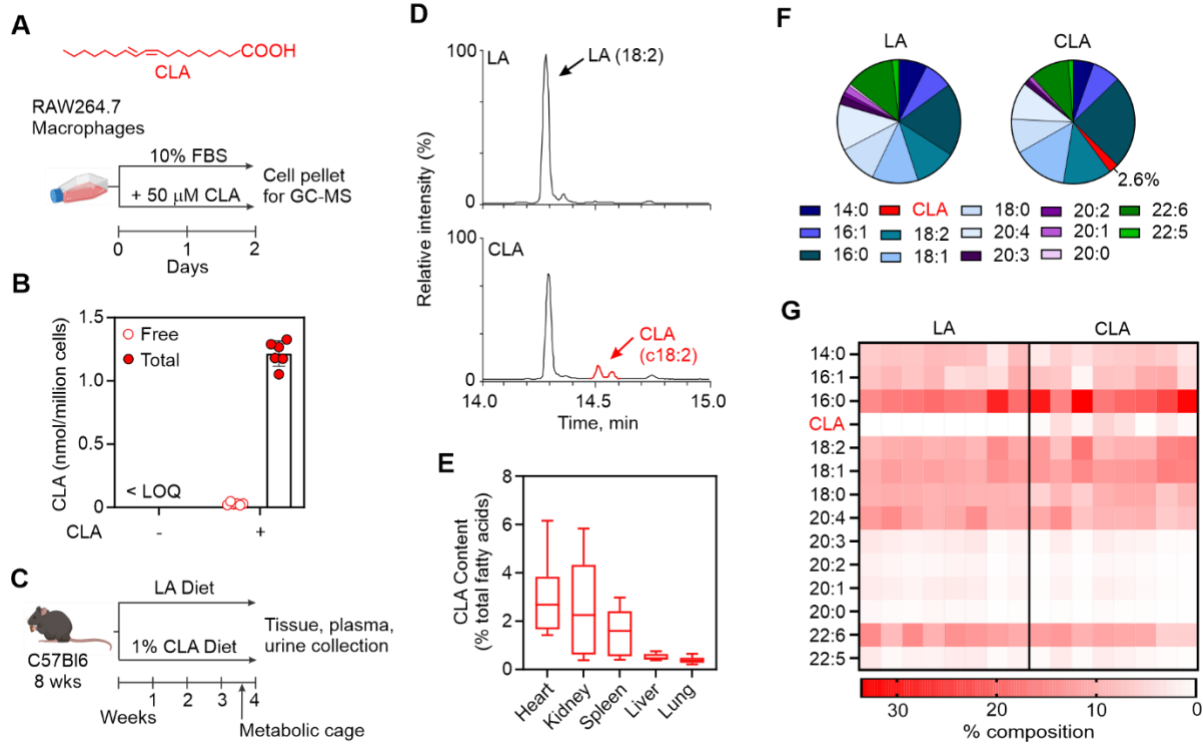


Figure 1. CLA supplementation primes cellular and in vivo systems for lipid nitration. A. Workflow for CLA enrichment in RAW264.7 macrophages. The structure for CLA is in red. **B.** Free and total levels of CLA in the cell pellet for control and CLA-supplemented conditions ($n = 6$). Representative result of three independent experiments. **C.** Mouse dietary intervention workflow. **D.** Representative GC-MS trace of control (LA diet) and CLA-supplemented kidney tissue for the mass range m/z 279-279.5. **E.** CLA enrichment in tissue from treated mice represented as a percentage of the total fatty acids ($n = 6-8$). **F.** Average fatty acid distribution for control (LA diet) and CLA-supplemented kidney tissue ($n = 7-8$). **G.** Individual mouse fatty acid enrichment for control and treated kidney tissue.

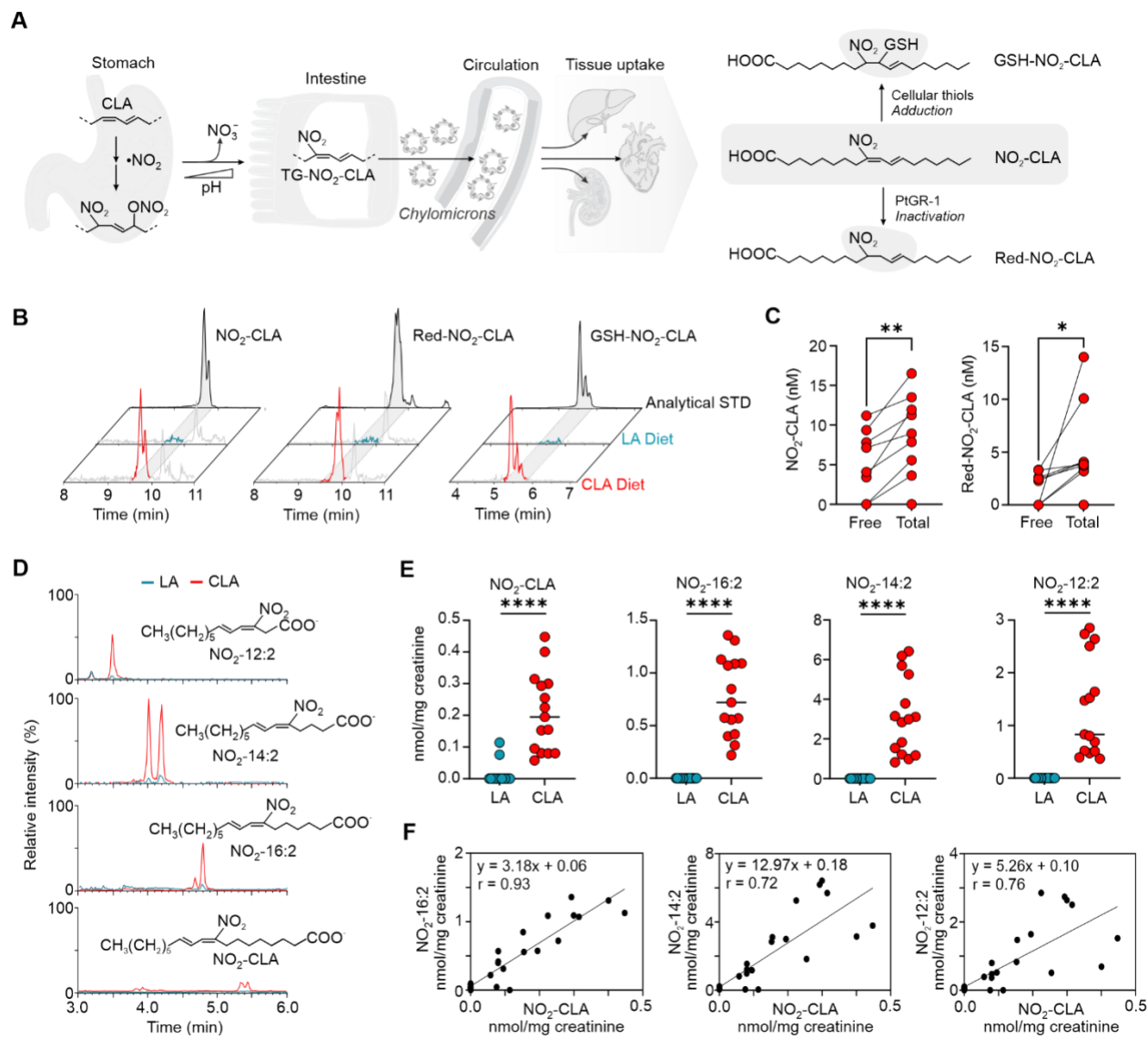


Figure 2. Gastric nitration establishes bioavailable NO₂-CLA. **A.** Schematic of CLA nitration, NO₂-CLA absorption, and metabolism. Acidic nitrite in the stomach drives the nitration of CLA-enriched triglycerides, initially forming a nitro-nitrate derivative (NO₂-ONO₂-CLA) that spontaneously decays into NO₂-CLA upon exiting the stomach because of the pH increase. Enterocytes package NO₂-CLA into triglycerides and export them in chylomicrons for tissue distribution, where the nitroalkene exerts its signaling actions, is stored in phospholipids, or metabolized into glutathione derivatives or inactive, reduced products. **B.** Representative chromatograms showing co-elution of analytical standards and NO₂-CLA (left), the inactive metabolite red-NO₂-CLA (middle), and GSH-NO₂-CLA (right) detected in plasma. **C.** Plasma concentration of free and total endogenous NO₂-CLA and red-NO₂-CLA (n=9). *P < 0.05, **P < 0.001 by paired t-test. **D.** Representative traces for NO₂-CLA and electrophilic β-oxidation metabolites detected in the mercury-treated urine from animals fed a diet rich in CLA (red) or LA (blue). **E.** Urine concentrations of NO₂-CLA and its β-oxidation metabolites (n=15-16). ****, P value < 0.0001 by unpaired t-test. **F.** Correlation analysis between NO₂-CLA and its metabolites by simple linear regression.

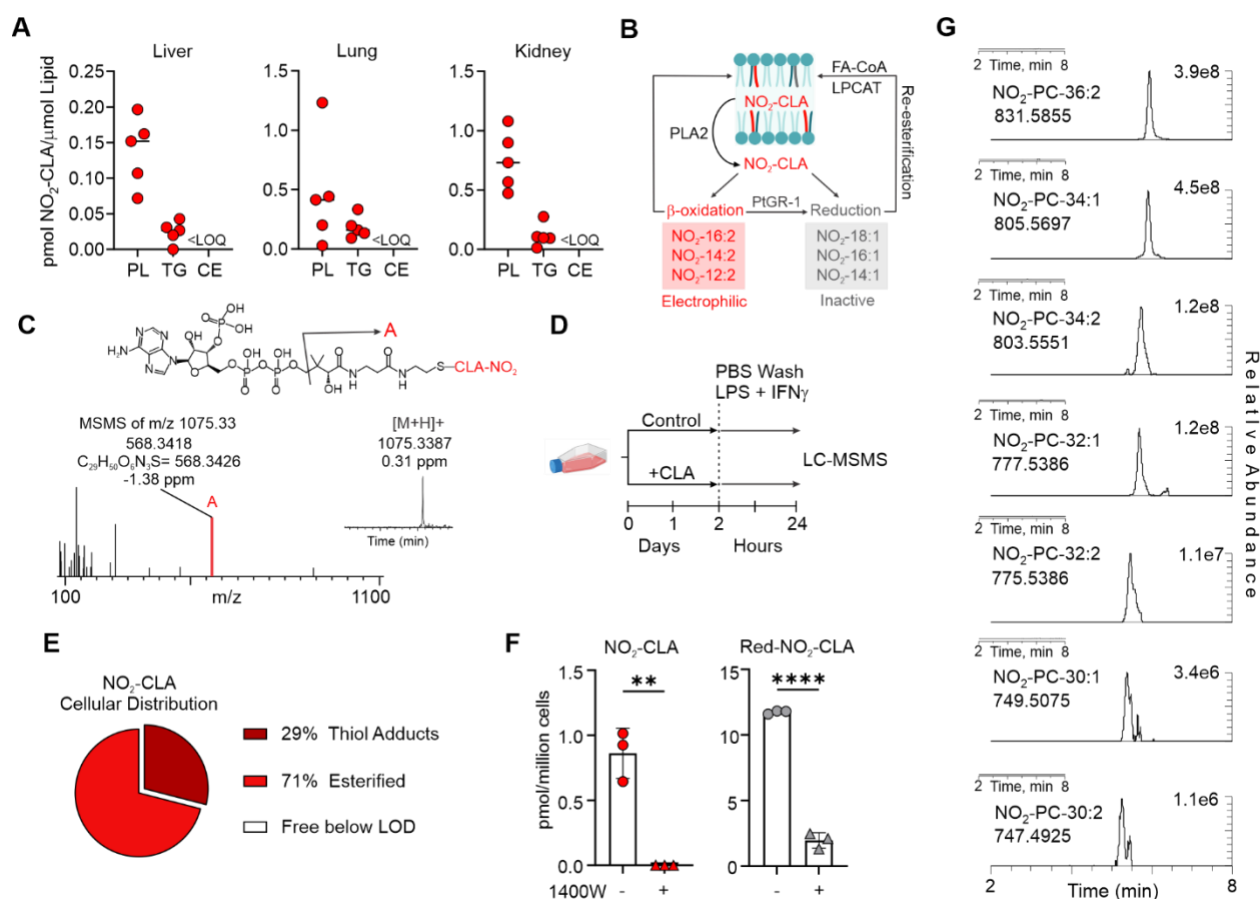


Figure 3. Phospholipids are biochemical cell capacitors that store endogenous fatty acid nitroalkenes. **A.** NO₂-CLA enrichment in phospholipids, triglycerides, and cholesterol esters after purification of each lipid class in selected tissues (n=5). **B.** Schematic of the Land's Cycle of membrane remodeling and the contribution of NO₂-FAs. **C.** Representative LC-HR-MS trace and MSMS fragmentation of NO₂-CLA-CoA adduct detected in cultured RAW264.7 macrophages. **D.** Experiment design of esterified-CLA nitration by LPS/IFN_γ activation of supplemented RAW264.7 macrophages. **E.** Cellular distribution of cell-generated NO₂-CLA in CLA-supplemented RAW264.7 macrophages after 24 hours of endotoxin challenge (n=6). Representative result from three independent experiments. **F.** Inhibition of total NO₂-CLA formation (free and esterified) in the presence of the iNOS inhibitor 1400W (100 μM) (n=3). Representative result from three independent experiments. **, P<0.01, ****, P<0.0001 by unpaired t-test. **G.** Representative LC-HR-MS traces of NO₂-PCs from LA- (inset) or CLA-supplemented RAW264.7 macrophages after 24 hours of LPS/IFN_γ stimulus.

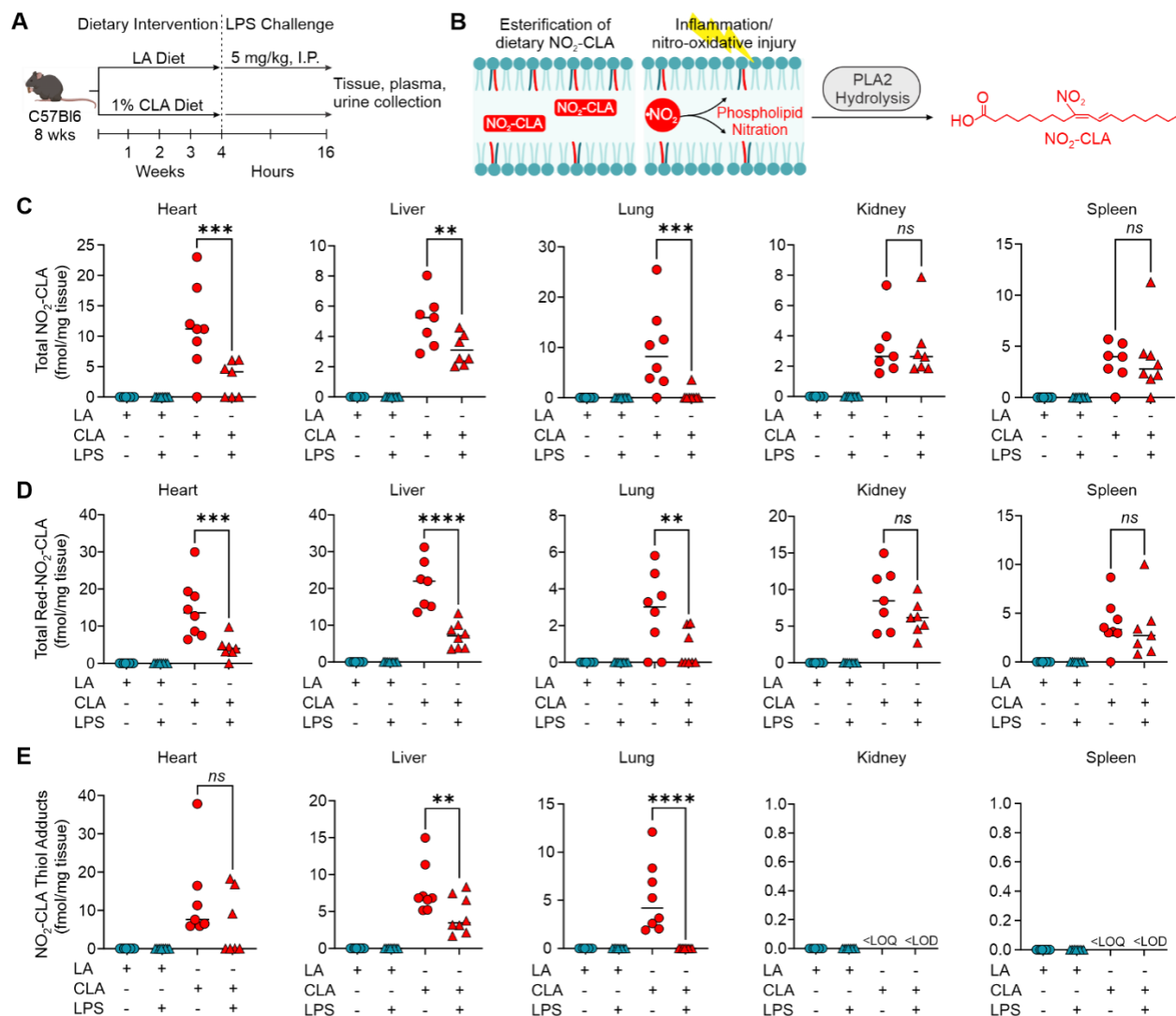


Figure 4. Endotoxemia favors the net release of $\text{NO}_2\text{-CLA}$. **A.** Workflow for *in vivo* dietary intervention followed by 16 hours of LPS challenge. **B.** Pathways contributing to the tissue availability of $\text{NO}_2\text{-CLA}$: diet-derived $\text{NO}_2\text{-CLA}$ is stored in phospholipids, and the nitration of esterified CLA occurs during inflammation. $\text{NO}_2\text{-CLA}$ derived from either pathway is susceptible to PLA2 hydrolysis during LPS challenge. **C-E.** Levels of total (**C**) $\text{NO}_2\text{-CLA}$, (**D**) red- $\text{NO}_2\text{-CLA}$, and (**E**) $\text{NO}_2\text{-CLA}$ thiol adducts detected in tissues from LA- or CLA-fed mice with or without LPS challenge ($n=7-8$). $\text{NO}_2\text{-CLA}$ and metabolic products are only detected in mice receiving the CLA diet. *, $P<0.05$, **, $P<0.01$, ***, $P<0.001$, ****, $P<0.0001$ versus CLA as determined by ANOVA and Dunnett's multiple comparisons test.

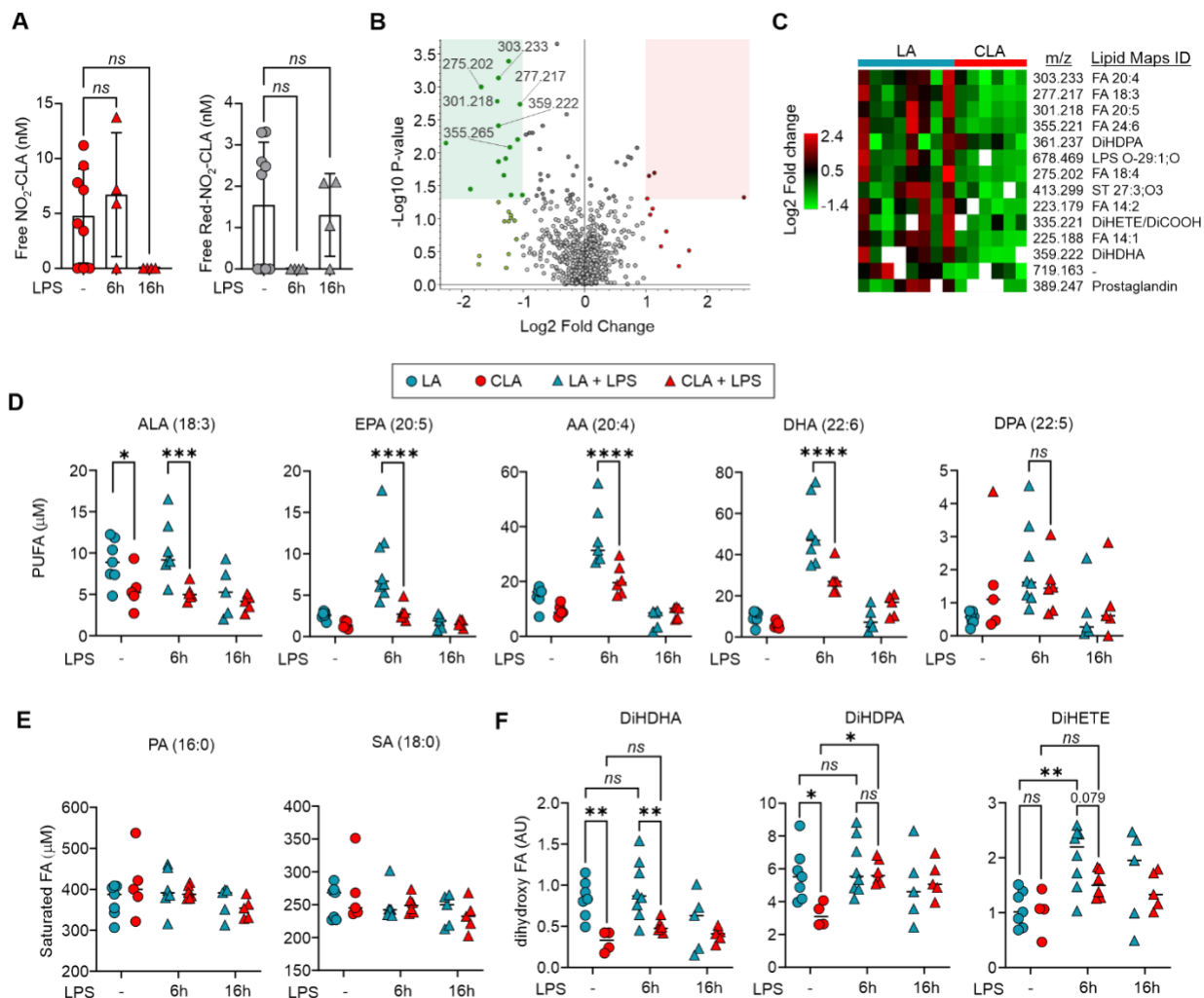


Figure 5. NO₂-CLA inhibits the release of sn-2 esterified fatty acids. **A.** Free NO₂-CLA and red-NO₂-CLA in plasma from CLA-fed control and LPS-challenged mice (n = 4-10). **B.** Volcano plot derived from lipidomic analysis showing the differential abundance of lipid species in plasma samples from LA- and CLA-fed mice after 6 hours of LPS challenge (n = 5-7). Several lipid species with significantly decreased abundance are indicated. **C.** Heat map comparing lipid species between LA- and CLA-fed groups. Significantly downregulated features in the CLA group were identified as fatty acids and dihydroxy fatty acids using the LIPID MAPS online database. White boxes indicate undetected lipid species. **D-F.** Plasma concentrations of free **(D)** PUFAs, **(E)** saturated fatty acids, and **(F)** dihydroxy fatty acids in CLA-fed mice at baseline and after 6 or 16h of LPS challenge. Statistical analysis was performed using two-way ANOVA and Tukey's multiple comparisons test. **, P<0.01, ***, P<0.001, ****, P<0.0001.

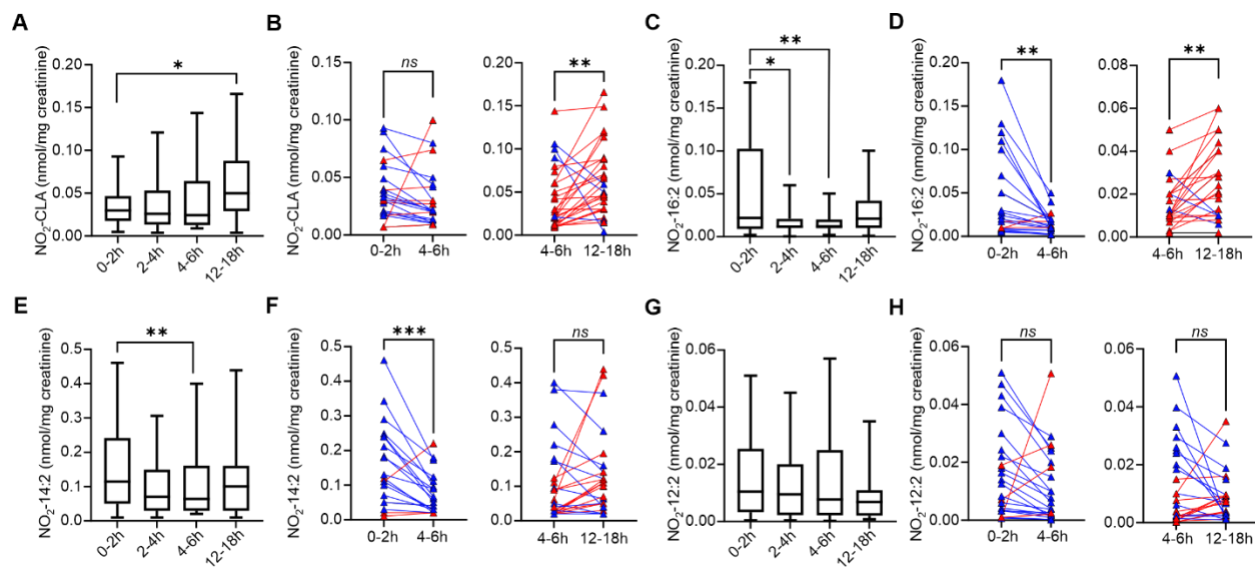


Figure 6. Urine accumulates excreted $\text{NO}_2\text{-CLA}$ after LPS administration. Urinary $\text{NO}_2\text{-CLA}$ (A) and β -oxidation metabolites (C, E, G) from human subjects at defined intervals post LPS administration ($n = 35$). Box and whisker plots show median, 25th to 75th percentiles, and range. *, $P < 0.05$, **, $P < 0.01$, ***, $P < 0.001$ versus 0–2-hour time-interval as determined by mixed-effects analysis and Dunnett's multiple comparisons test. Individual-level changes in urinary $\text{NO}_2\text{-CLA}$ (B) and metabolites (D, F, H) for the first and second half of endotoxin challenge. Subjects without samples for both time intervals were excluded from the paired comparison. 21 subjects are represented in the paired analysis between 0–2 hours vs. 4–6 hours, whereas 27 subjects are represented in 4–6 hours vs. 12–18 hours. Blue lines indicate a negative slope and red a positive slope. *, $P < 0.05$, **, $P < 0.01$, ***, $P < 0.001$ as determined by paired t-test.

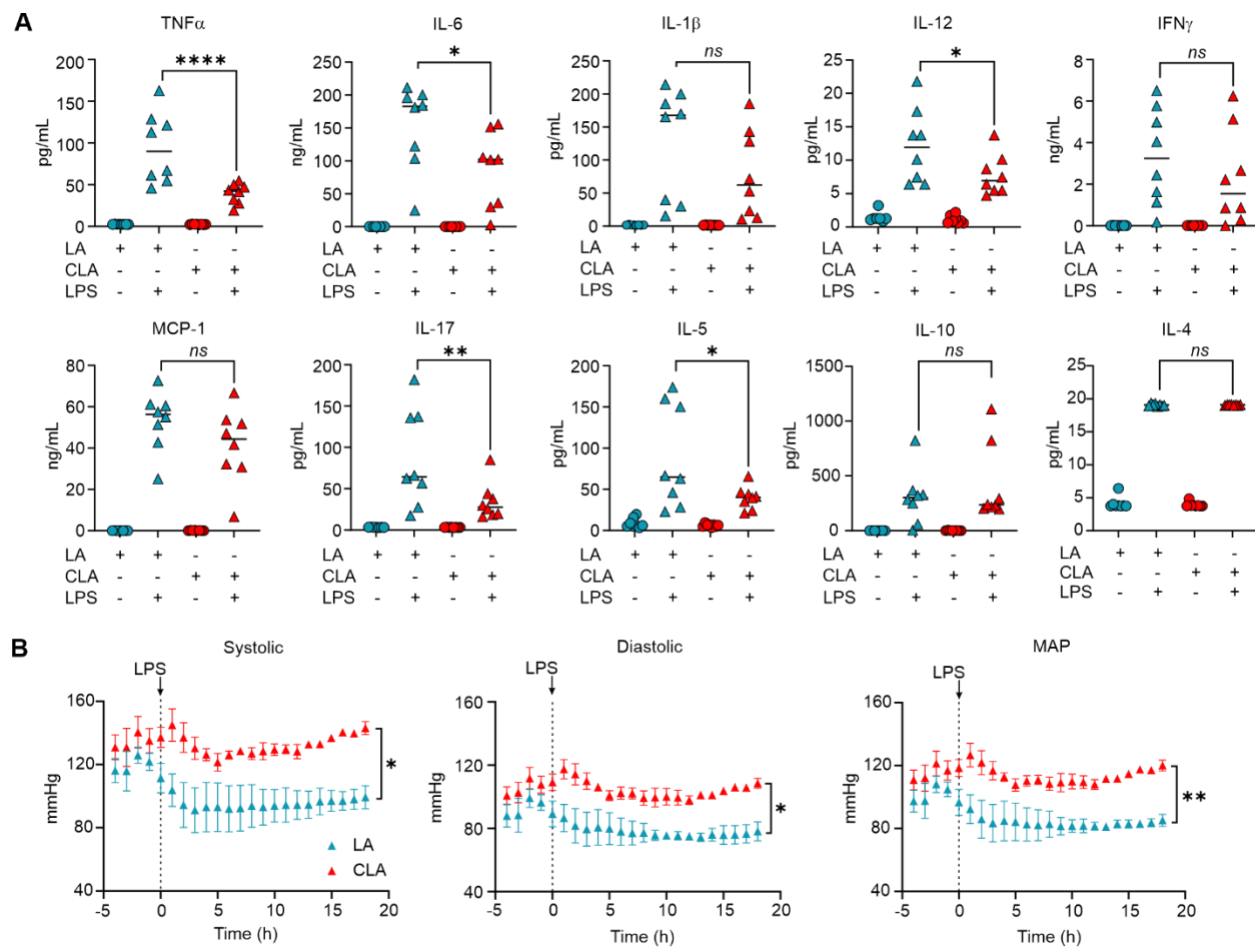


Figure 7. Endogenous NO₂-CLA attenuates pro-inflammatory cytokines and modulates vascular responses. A. Multiplex analysis of plasma cytokines measured 6 hours after saline or LPS administration in LA- or CLA-fed mice (n=6-8). Statistical analysis by one-way ANOVA and Dunnett's multiple comparisons test. *, P<0.05, **, P<0.01, ***, P<0.001, ****, P<0.0001 versus LA+LPS. **B.** Blood pressure recordings by telemetry in LA- and CLA-fed mice during the LPS challenge (n=4 per group). MAP = mean arterial pressure. Statistical analysis was performed using two-way ANOVA and Sídák's multiple comparisons test. Interaction P-value plotted. *, P<0.05, **, P<0.01

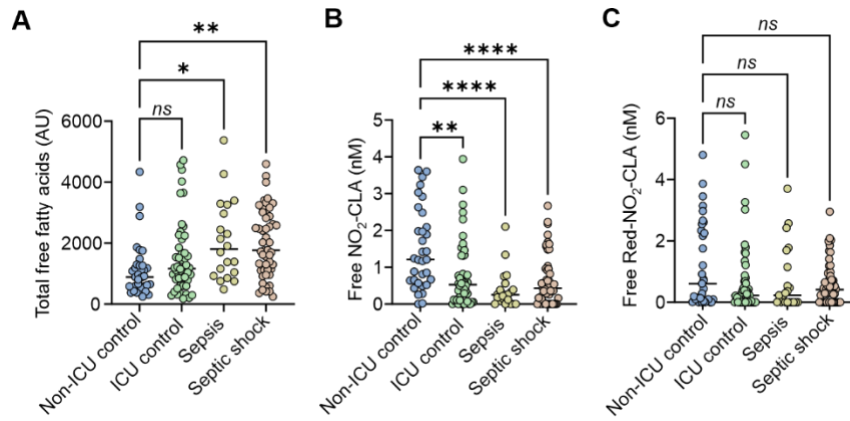


Figure 8. Plasma NO₂-CLA levels are lower in humans with septic shock. **A.** Total fatty acids, **B.** free NO₂-CLA, and **C.** free red-NO₂-CLA measured in plasma from healthy controls, ICU patients without sepsis, and patients with septic shock. Each dot represents an individual subject (n = 21-53). *, P<0.05, **, P<0.01, ***, P<0.001, ****, P<0.0001 from one-way ANOVA and Tukey's multiple comparisons.

TABLES

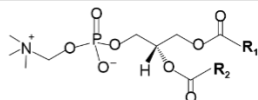
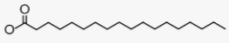
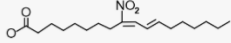
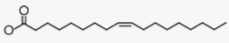
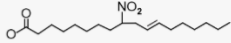
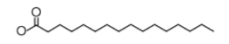
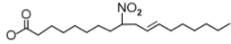
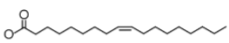
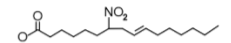
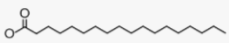
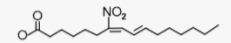
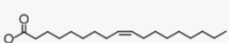
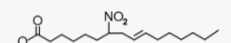

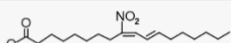

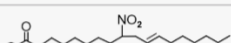

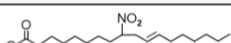

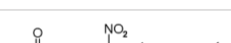
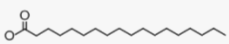
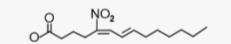
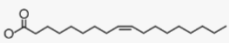
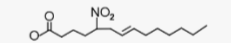
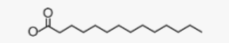
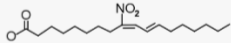
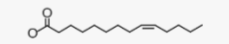
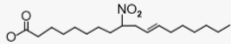
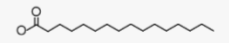
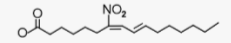
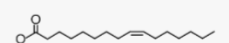
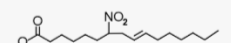
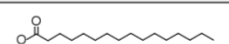
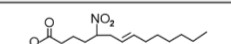

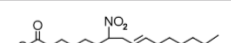

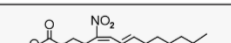

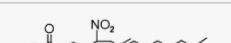

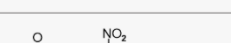
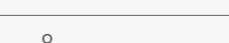
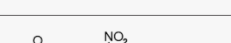
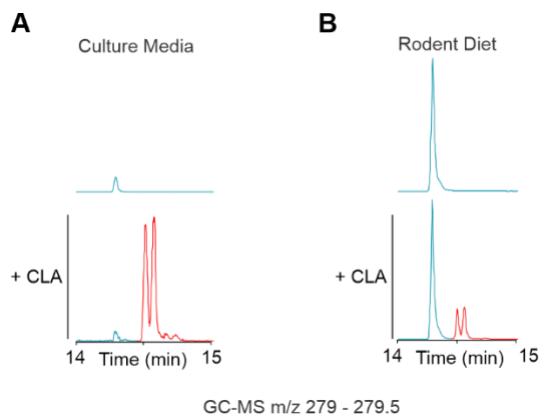
Chemical Formula	Analyte	Positive ion mode [M+H] ⁺		Negative ion mode [M+HCOO] ⁻			
		Theoretical mass	Experimental mass	Theoretical mass	Experimental mass	R ₁	R ₂
NO ₂ -PC-36:2 C ₄₄ H ₈₃ O ₁₀ N ₂ P	PC(18:0/NO ₂ -18:2)	831.5858	831.5855	875.5762	875.5772		
	PC(18:1/NO ₂ -18:1)						
NO ₂ -PC-34:1 C ₄₂ H ₈₁ O ₁₀ N ₂ P	PC(16:0/NO ₂ -18:1)	805.5702	805.5697	849.5605	849.5618		
	PC(18:0/NO ₂ -16:1)						
NO ₂ -PC-34:2 C ₄₂ H ₇₉ O ₁₀ N ₂ P	PC(18:0/NO ₂ -16:2)	803.5545	803.5551	847.5449	847.5456		
	PC(18:1/NO ₂ -16:1)						
	PC(16:0/NO ₂ -18:2)						
	PC(16:1/NO ₂ -18:1)						
NO ₂ -PC-32:1 C ₄₀ H ₇₇ O ₁₀ N ₂ P	PC(14:0/NO ₂ -18:1)	777.5389	777.5386	821.5292	821.5303		
	PC(16:0/NO ₂ -16:1)						
NO ₂ -PC-32:2 C ₄₀ H ₇₅ O ₁₀ N ₂ P	PC(18:0/NO ₂ -14:2)	775.5232	775.5235	819.5136	819.5157		
	PC(18:1/NO ₂ -14:1)						
	PC(14:0/NO ₂ -18:2)						
	PC(14:1/NO ₂ -18:1)						
	PC(16:0/NO ₂ -16:2)						
	PC(16:1/NO ₂ -16:1)						
NO ₂ -PC-30:1 C ₃₈ H ₇₃ O ₁₀ N ₂ P	PC(16:0/NO ₂ -14:1)	749.5076	749.5075	793.4979	793.4999		
	PC(14:0/NO ₂ -16:1)						
NO ₂ -PC-30:2 C ₃₈ H ₇₁ O ₁₀ N ₂ P	PC(16:0/NO ₂ -14:2)	747.4919	747.4925	791.4823	791.4838		
	PC(16:1/NO ₂ -14:1)						
	PC(14:0/NO ₂ -16:2)						
	PC(14:1/NO ₂ -16:1)						

Table 1. Summary of the NO₂-PCs detected in activated RAW264.7 macrophages. High-resolution experimental masses obtained in positive and negative ion mode are shown with the corresponding theoretical mass for each PC with esterified NO₂-CLA metabolites. Proposed structures for the sn-1 and sn-2 positions of the NO₂-PC are indicated.

SUPPLEMENTARY FIGURES

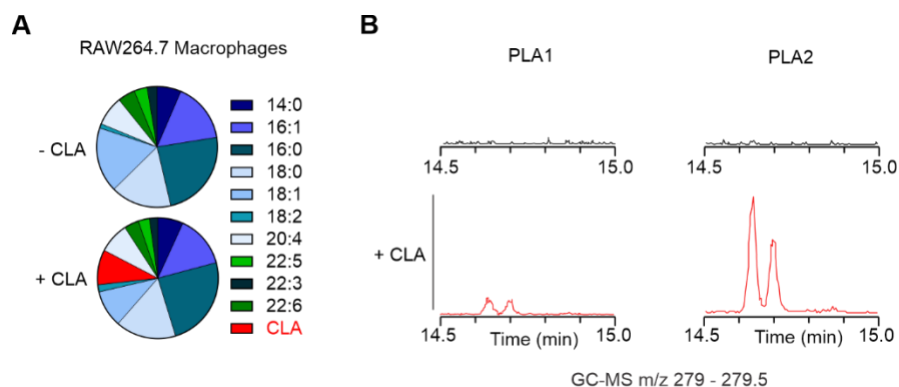
Nitrated fatty acids are cell membrane biochemical capacitors that regulate inflammation

Nicole Colussi¹, Sonia R. Salvatore¹, Matias M. Vazquez¹, Maria V. Gutierrez^{2,3}, Scott Hahn^{1,4}, Karina Ricart⁵, Felipe Vendrame⁵, Matias Badino¹, Agustina Schopfer¹, Dario A. Vitturi⁵, **Luis Villacorta**¹⁰, Rakesh P. Patel⁵, Amit Gaggar^{5,6}, Carsten Skarke⁷, Adam C. Straub^{1,4}, Francisco J. Schopfer^{*1,4,8,9}

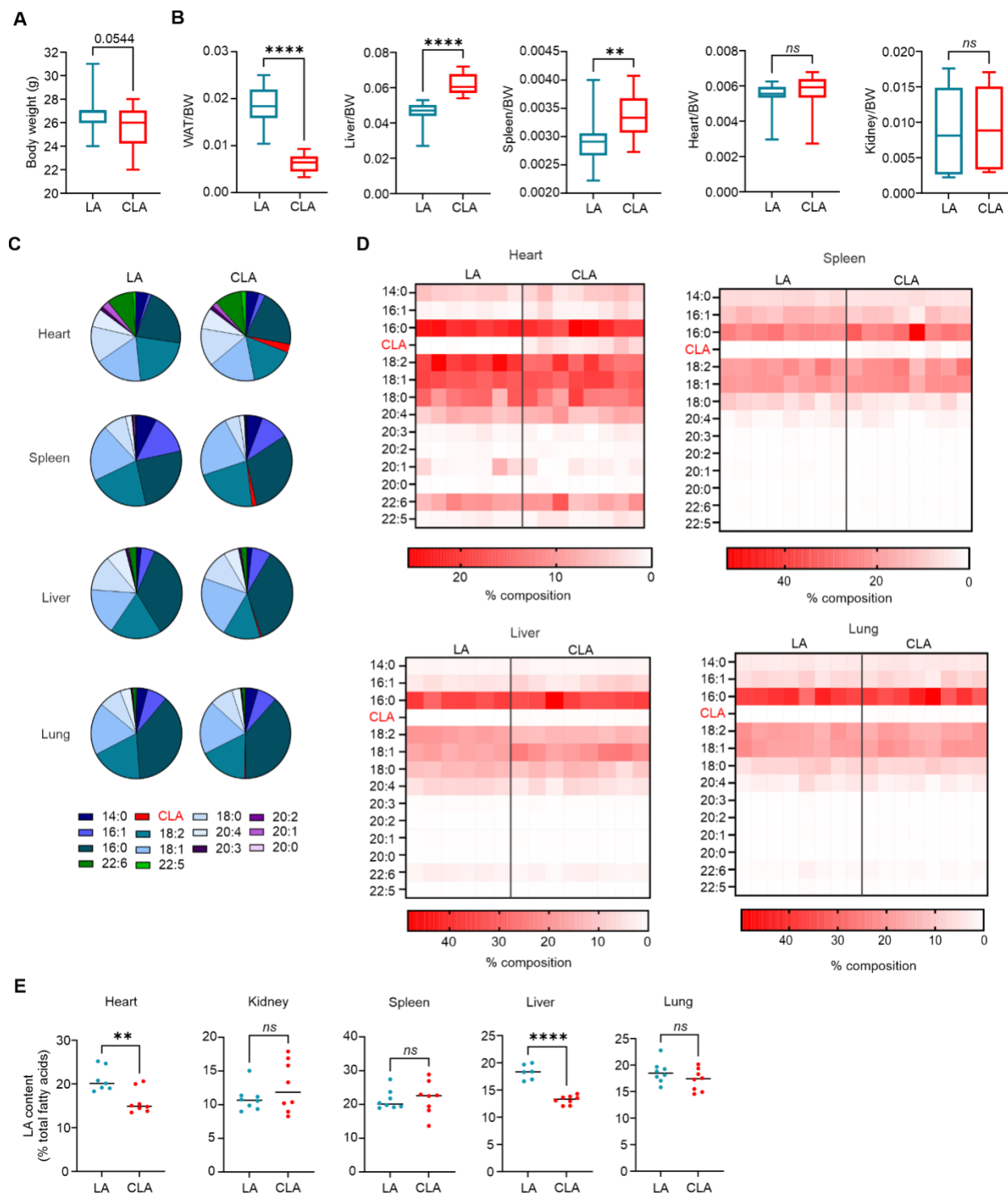


Supplementary Figure 1. Endogenous CLA is absent from cell culture and in vivo models.

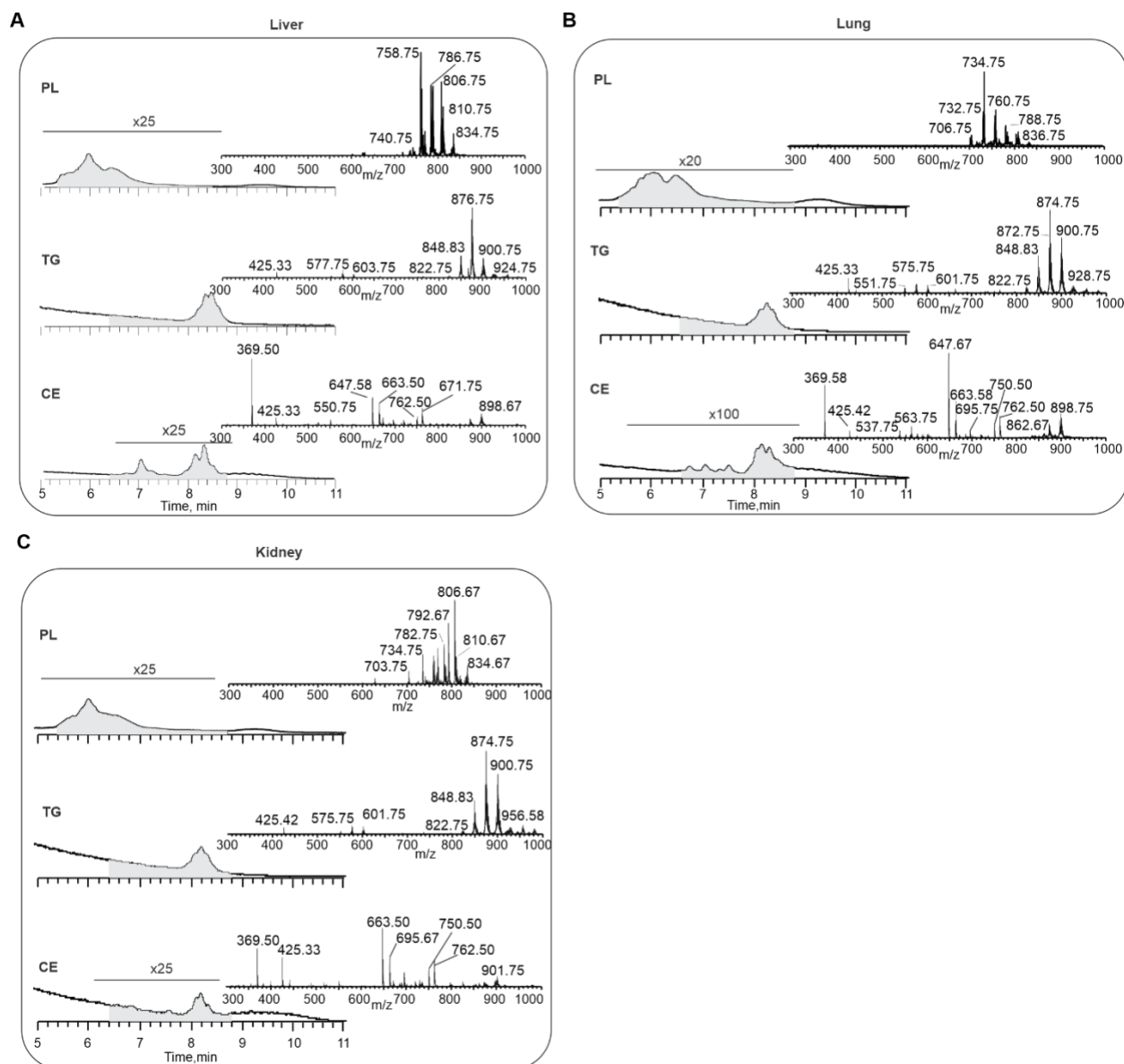
Gas chromatography–mass spectrometry (GC-MS) analysis (m/z: 279–279.5) showing no detectable CLA in **A**) standard cell culture media and **B**) rodent diet. Top chromatography traces represent un-supplemented conditions, with linoleic acid (blue) as the only octadecadienoic acid (18:2) isomer. Bottom traces show CLA addition (red) to culture media (50 μ M) and rodent diet (1% CLA).



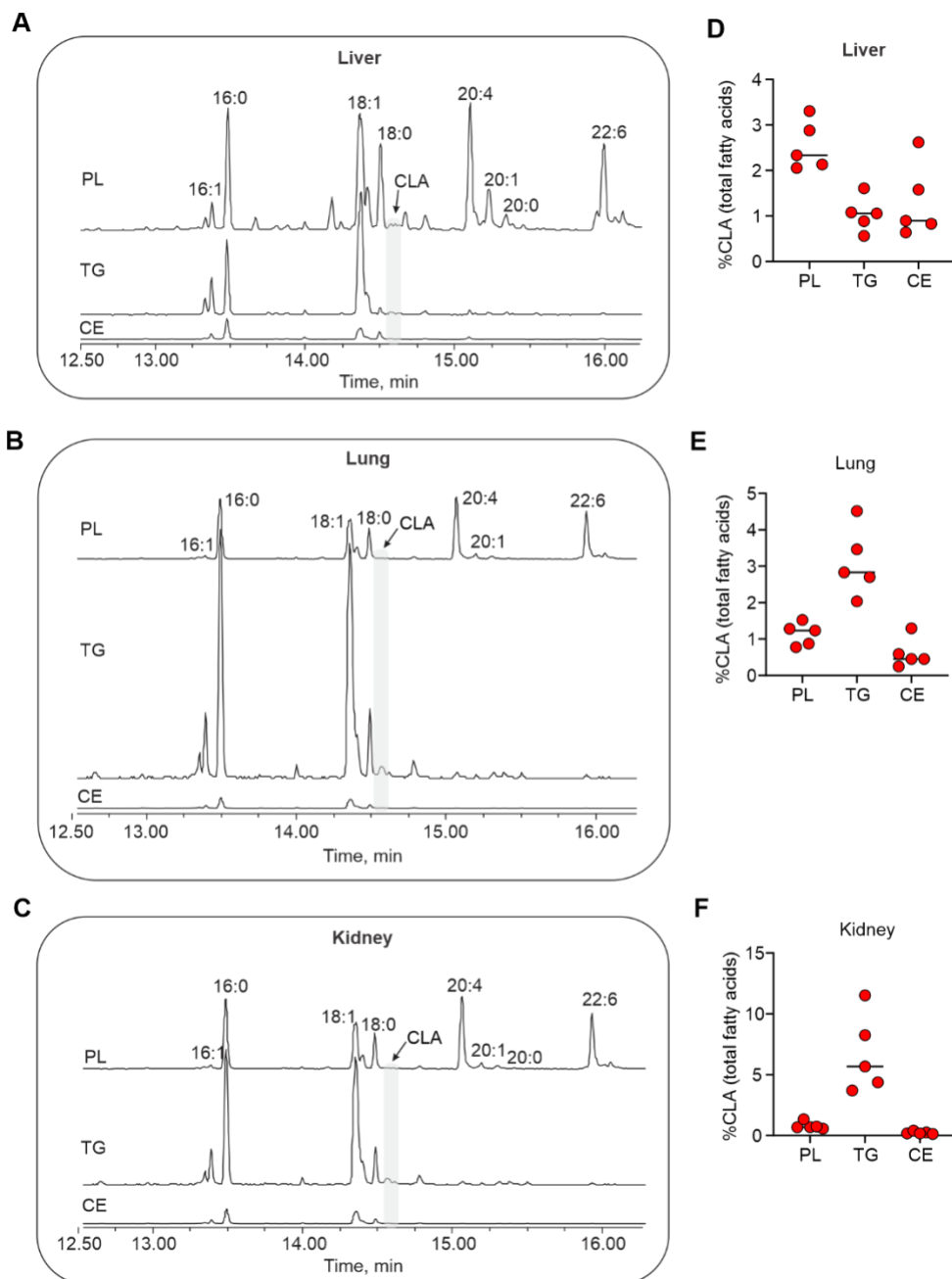
Supplementary Figure 2. Supplementation of CLA to RAW264.7 macrophages leads to uptake in the fatty acid profile and phospholipids. A. Fatty acid profile distribution in cultured RAW264.7 macrophages after supplementation of 50 μM CLA (n=3). Representative experiment of three independent trials. **B.** Representative GC-MS traces (m/z: 279–279.5) of free CLA after phospholipase hydrolysis of phospholipid fractions from control (top trace, black) and CLA supplemented RAW264.7 macrophages (bottom trace, red).



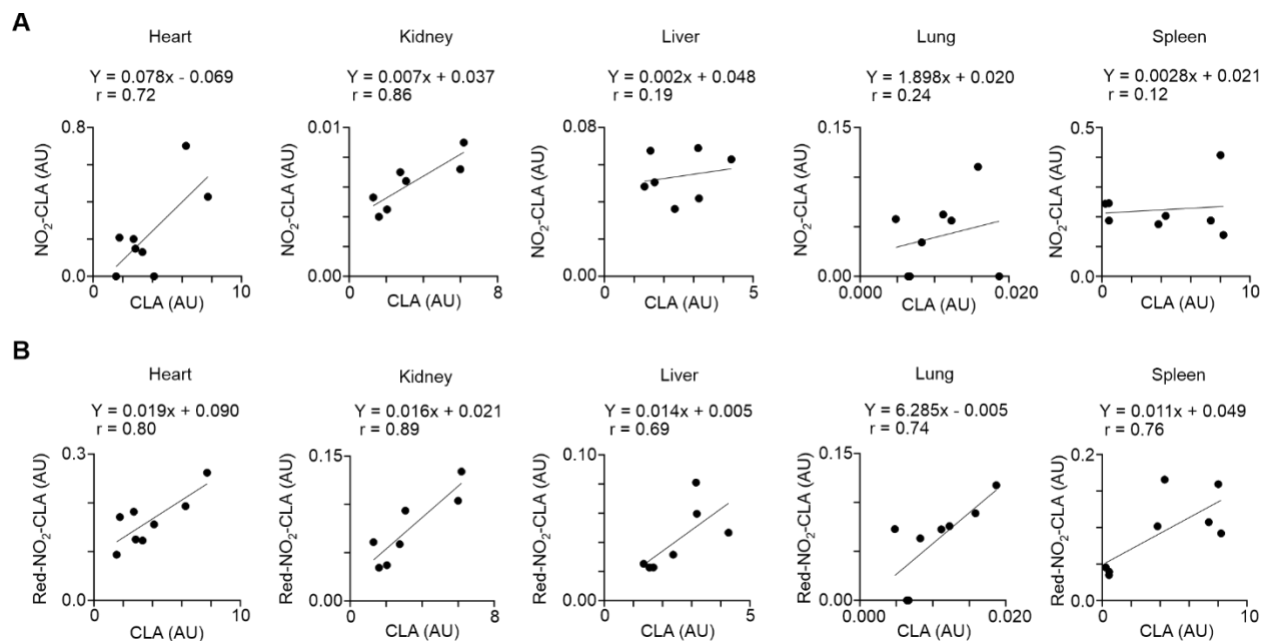
Supplementary Figure 3. Effect of CLA on body composition and fatty acid distribution in mice. A-B. A) Body weight and **B)** normalized tissue weights of mice fed either a LA (control) or 1%CLA diet for 4 weeks (n=8). Box and whiskers plot indicate median, 25th to 75th percentiles and range. **, $P < 0.01$, ****, $P < 0.0001$ by unpaired t test. **C.** Fatty acid distribution for LA or CLA-fed mice. (n = 6-8). **D.** Heat map comparison of individual mouse tissue fatty acid enrichment profiles in LA and CLA diet groups (n = 6-8). **E.** LA levels expressed as a percentage of total fatty acids in LA or CLA diet tissue (n = 6-8).



Supplementary Figure 4. Confirmation of lipid fractionation by HPLC-CAD-MS analysis. Representative charged aerosol detector (CAD) traces for PL, TG, and CE fractions in (A) liver, (B) lung, and (C) kidney. Mass spectra for each of the fractions are filtered for the grayed-out area in the CAD trace.

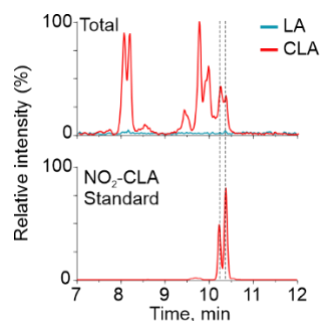


Supplementary Figure 5. CLA incorporation into different lipid classes after dietary supplementation. A-C. Representative total ion chromatograms (TIC) for liver, lung, and kidney tissue after hydrolysis of purified lipid fractions. Fatty acid intensities are normalized across phospholipid, triglyceride, and cholesterol ester fractions for the respective tissue. **D-F.** Abundance of CLA in each lipid fraction shown as a percentage of the total fatty acids.

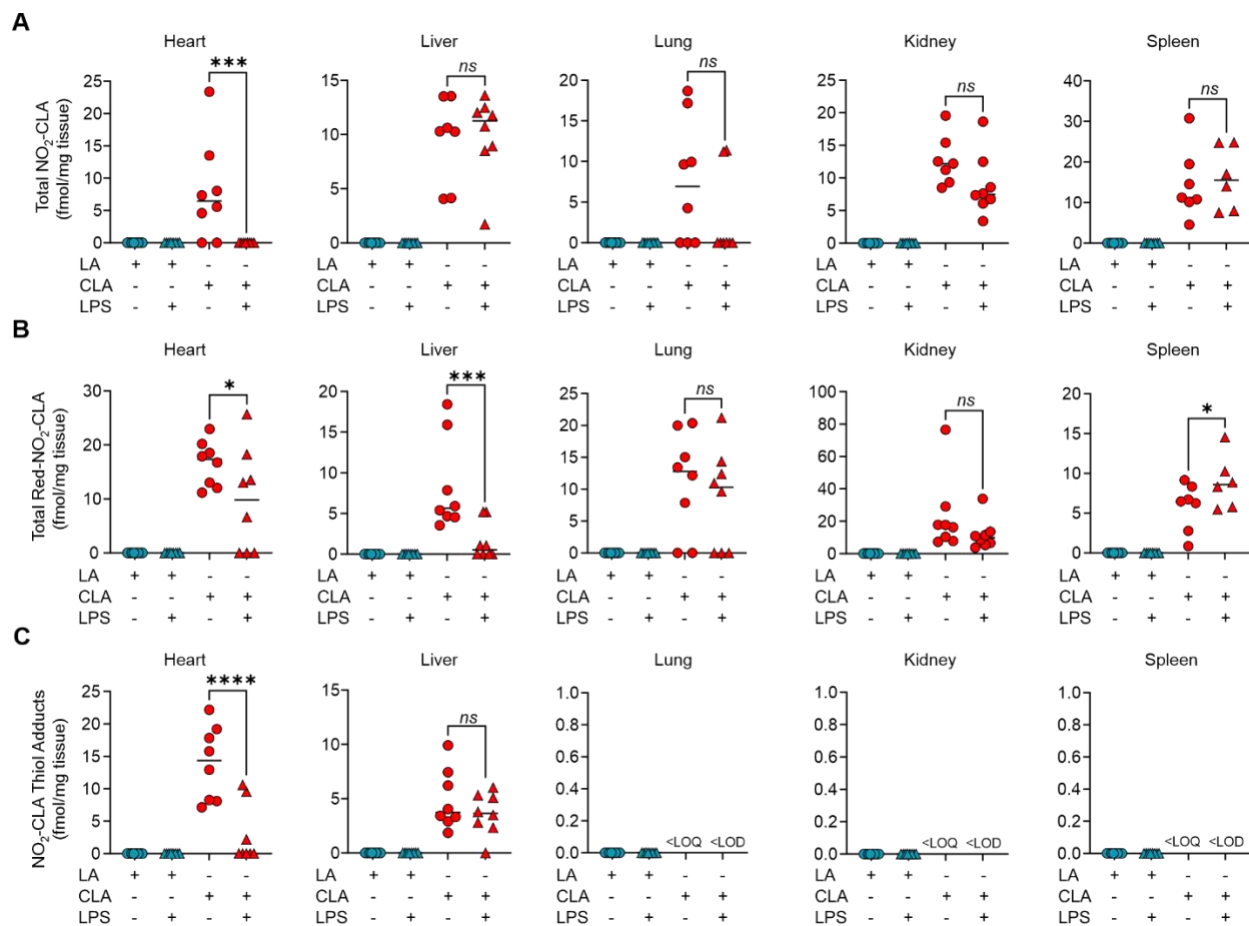


Supplementary Figure 6. NO₂-CLA tissue uptake and metabolism is independent of CLA. Correlation plots between tissue levels of **A)** CLA vs. NO₂-CLA and **B)** CLA vs. the inactivated metabolite red-NO₂-CLA.

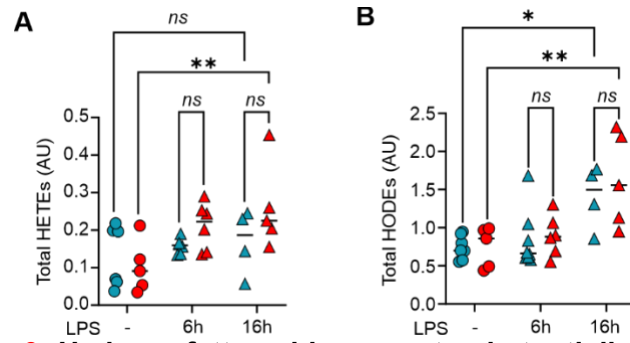
Supplementary Figure 7. NO₂-supplemented RAW264.7
 LC-MSMS trace for NO₂-CLA
 CLA-supplemented (red)
 LPS/IFN γ stimulus for 24 hours. Traces represent total NO₂-CLA levels in the cells measured after acidic hydrolysis. A synthetic standard for NO₂-CLA was used to correctly identify the product peak from the chromatogram.



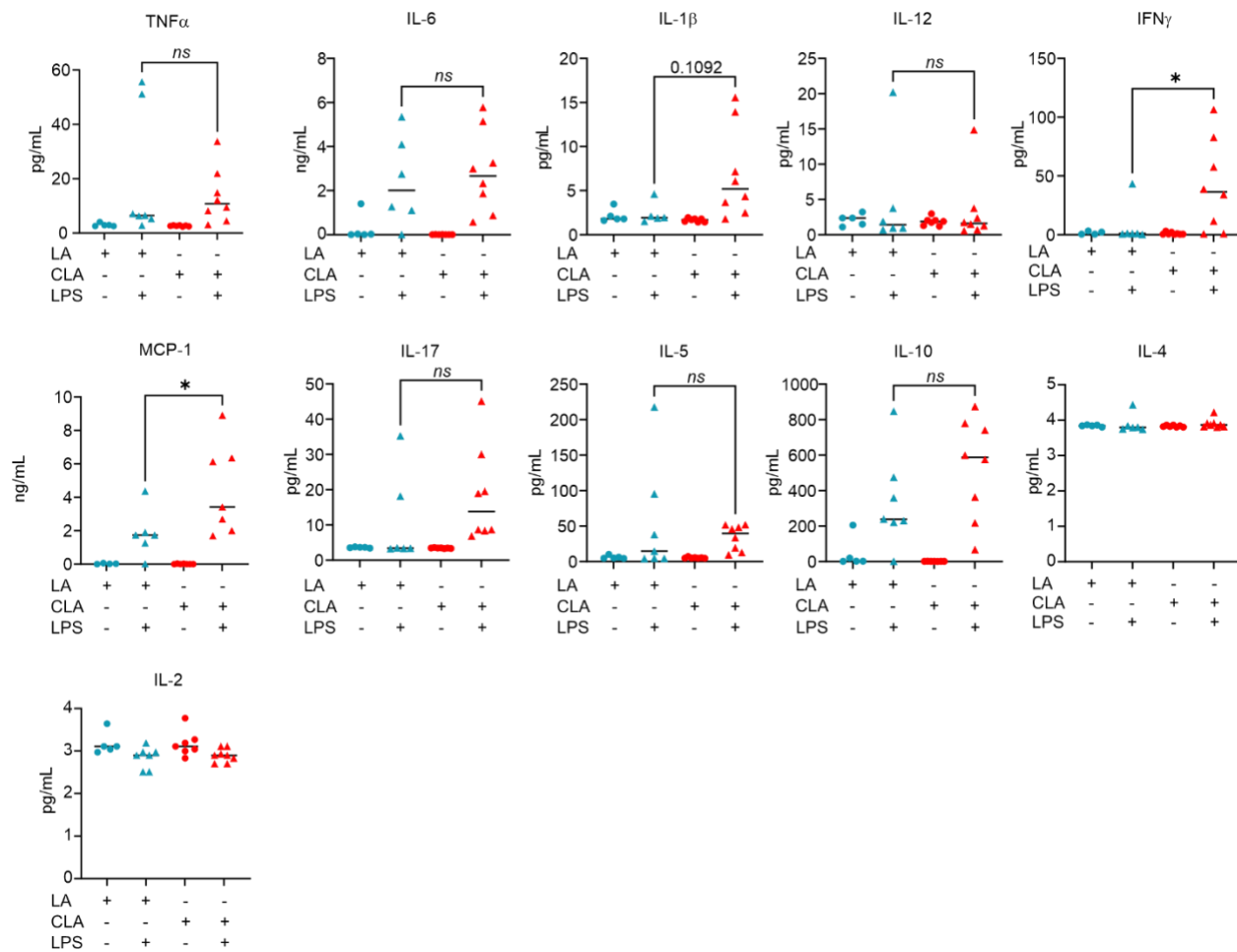
CLA does not form in LA-macrophages. Representative (MRM: 324/46) in LA- (blue) or RAW264.7 macrophages after



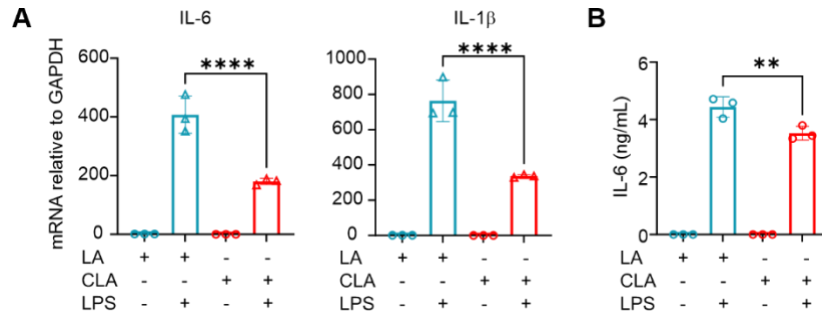
Supplementary Figure 8. Total NO₂-CLA and its metabolic products trend lower after 6 hours of LPS challenge. **A.** Total NO₂-CLA, **B.** red-NO₂-CLA, and **C.** NO₂-CLA thiol adducts levels detected in tissue from LA- or CLA-fed mice and LPS-challenged (n=7-8). NO₂-CLA and metabolic products are only detected in mice fed the CLA-supplemented diet. *, P<0.05, **, P<0.01, ***, P<0.001, ****, P<0.000 versus CLA as determined ANOVA and Dunnett's multiple comparisons test.



Supplementary Figure 9. Hydroxy fatty acids are not substantially upregulated following LPS challenge. Total levels of **A)** HETEs and **B)** HODEs detected in plasma from baseline and LPS-challenged mice fed either an LA (blue) or CLA (red) diet. (n= 5-7). *, P<0.05, **, P<0.01 by two-way ANOVA and Tukey's multiple comparisons.



Supplementary Figure 10. Pro-inflammatory cytokines are reduced at 16 hours after LPS challenge. Multiplex analysis of pro-inflammatory cytokines measured in the plasma from mice fed LA or CLA diets following 16 hours of saline or LPS administration (n = 5 -8). *, P<0.05 versus LA+LPS as determined by one-way ANOVA and Dunnett's multiple comparisons test.



Supplementary Figure 11. Macrophage-generated NO₂-CLA inhibits **A)** IL-6 and IL-1 β expression after 16 hours of LPS stimulation and **B)** IL-6 secretion after 6 hours of LPS stimulation in RAW264.7 macrophages. Representative data from three independent experiments. **, P<0.01, ****, P<0.0001 determined by one-way ANOVA and Tukey's comparison.